

AD-A054 376

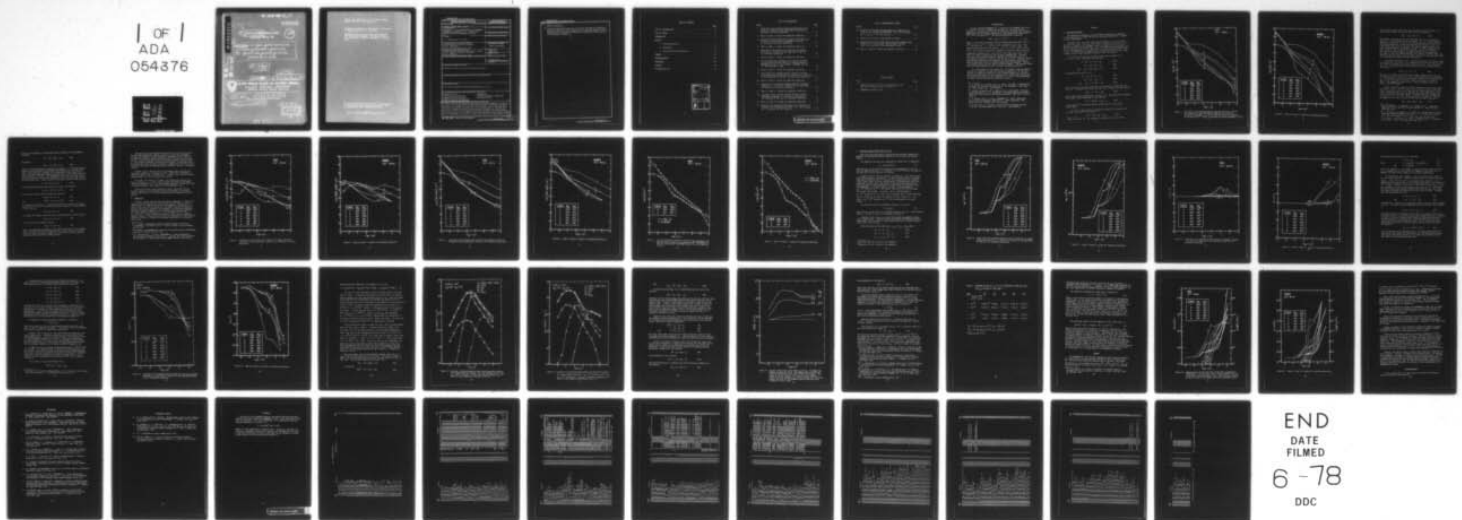
ARMY ARMAMENT RESEARCH AND DEVELOPMENT COMMAND ABERD--ETC F/G 4/1  
BENCHMARK-76: MODEL COMPUTATIONS FOR DISTURBED ATMOSPHERIC COND--ETC(U)  
MAR 78 J M HEIMERL, F E NILES  
ARBRL-TR-02051

SBIE-AD-E430 022

NL

UNCLASSIFIED

1 OF 1  
ADA  
054376



AD A 054376

FOR FURTHER TRAN

AD-E430022

9 TECHNICAL REPORT ARBRL-TR-02051  
(Supersedes IMR No. 510)

12

BENCHMARK-76: MODEL COMPUTATIONS FOR  
DISTURBED ATMOSPHERIC CONDITIONS.  
III. RESULTS FOR SELECTED EXCITATION  
PARAMETERS AT 60 KM.

10 J. M. Heimerl  
F. E. Niles

12 52p.

11 Mar 78

14 ARBRL-TR-02051



US ARMY ARMAMENT RESEARCH AND DEVELOPMENT COMMAND  
BALLISTIC RESEARCH LABORATORY  
ABERDEEN PROVING GROUND, MARYLAND

18 SBIE

19 AD-E430022

Approved for public release; distribution unlimited.

16 11161102B53A

DDC  
RECEIVED  
MAY 20 1978  
REGISTERED  
B

393 471

Destroy this report when it is no longer needed.  
Do not return it to the originator.

Secondary distribution of this report by originating  
or sponsoring activity is prohibited.

Additional copies of this report may be obtained  
from the National Technical Information Service,  
U.S. Department of Commerce, Springfield, Virginia  
22161.

The findings in this report are not to be construed as  
an official Department of the Army position, unless  
so designated by other authorized documents.

The use of trade names or manufacturers' names in this report  
does not constitute endorsement of any commercial product.



UNCLASSIFIED

SECURITY CLASSIFICATION OF THIS PAGE(When Data Entered)

Item 20, Continued:

cases and computations were made for daytime and nighttime conditions. Selected results and limited comparisons are reported together with the variations of the computed equivalent rate coefficients with time and with ionization conditions.

UNCLASSIFIED

SECURITY CLASSIFICATION OF THIS PAGE(When Data Entered)

# TABLE OF CONTENTS

	Page
LIST OF ILLUSTRATIONS. . . . .	5
LIST OF TABLES . . . . .	6
INTRODUCTION . . . . .	7
RESULTS	
A. Selected Densities. . . . .	8
B. Comparison. . . . .	13
C. Equivalent Rate Coefficients. . . . .	20
SUMMARY. . . . .	36
ACKNOWLEDGEMENT. . . . .	39
REFERENCES . . . . .	40
APPENDIX . . . . .	42
DISTRIBUTION LIST. . . . .	53

ACCESSION for		
NTIS	White Section	<input checked="" type="checkbox"/>
DCC	Dist Section	<input type="checkbox"/>
UNANNOUNCED		<input type="checkbox"/>
JUSTIFICATION		
BY		
DISTRIBUTION/AVAILABILITY CODES		
Dist.	AVAIL.	SPECIAL
A		

# LIST OF ILLUSTRATIONS

Figure	Page
1. Logarithm of the computed daytime electron density at 60 km as a function of the logarithm of time for six different excitation conditions. . . . .	9
2. Same as Figure 1, except for nighttime conditions. . . . .	10
3. Logarithm of the daytime total negative ion density at 60 km as a function of the logarithm of time for six different ionization conditions. . . . .	14
4. Same as Figure 3, except for nighttime conditions. . . . .	15
5. Logarithm of the daytime total positive ion density at 60 km as a function of the logarithm of time for six ionization conditions. . . . .	16
6. Same as Figure 5, except for nighttime conditions. . . . .	17
7. For two excitation conditions at 60 km the logarithm of the daytime electron density as computed by BRL's BENCHMARK-76 code (·) and Schiebe's DAIRCHEM code (X) vs. the logarithm of time. . . . .	18
8. Same as Figure 7, except for nighttime conditions. . . . .	19
9. Logarithm of the computed daytime effective electron-ion recombination coefficient, $\alpha_d$ , at 60 km as a function of the logarithm of time for six ionization conditions . . .	21
10. Same as Figure 9, except for nighttime conditions. . . . .	22
11. Logarithm of the computed daytime effective attachment frequency, A, at 60 km as a function of the logarithm of time for six ionization conditions. . . . .	23
12. Same as Figure 11, except for nighttime conditions . . . . .	24
13. Logarithm of the computed daytime effective electron detachment frequency, D, at 60 km as a function of the logarithm of time for six ionization conditions. . . . .	27
14. Same as Figure 13, except for nighttime conditions . . . . .	28
15. Histories of selected daytime negative ion densities at 60 km for the excitation conditions: $Q_0 = 10^6$ ion-pairs $\text{cm}^{-3}\text{s}^{-1}$ and $N_0 = 10^8 \text{ cm}^{-3}$ (Case 6) . . . . .	30

# LIST OF ILLUSTRATIONS (CONTD)

Figure	Page
16. Histories of selected daytime negative ion densities at 60 km for the excitation conditions: $Q_0 = 10^6$ ion-pairs $\text{cm}^{-3}\text{s}^{-1}$ and $N_0 = 10^{11} \text{ cm}^3$ (Case 4) . . . . .	31
17. History of the nitric oxide density at 60 km . . . . .	33
18. Composite plot of the logarithm of the total recombination coefficient, $\psi$ (solid line), and of $Q/[e]^2$ (dashed line), as a function of the logarithm of time. . . . .	37
19. Same as Figure 15, except for nighttime conditions . . . . .	38

# LIST OF TABLES

Table	Page
1. Computed values of $D \text{ (s}^{-1}\text{)}$ as a function of time and value of $k_{129}$ for Case 6 and Case 4. . . . .	35
A. BENCHMARK-76 Reaction Set. . . . .	43

## INTRODUCTION

We have employed BENCHMARK-76, a version of the AIRCHEM<sup>1</sup> code with a 64 species set and a nominal 496 reaction set, to obtain species densities as a function of time at an altitude of 60 km for the following conditions. For the prompt ionization,  $N_0$  was assigned the values  $10^{11}$ ,  $10^{10}$  or  $10^8$  ion-pairs  $\text{cm}^{-3}$ . The delayed ionization is given by

$$Q(t) = Q_0 (1 + t)^{-1.2}, \quad (1)$$

where  $t$  is the time in seconds, and  $Q_0$  assigned the values  $10^6$ ,  $10^8$  or  $10^{10}$  ion-pairs  $\text{cm}^{-3} \text{ s}^{-1}$ , subject to the constraint  $|Q_0| < |N_0|$ . The relative distribution of the species:  $N_2^+$ ,  $O_2^+$ ,  $N^+$ ,  $O^+$ ,  $N(^4S)$ ,  $N(^2D)$ ,  $O(^3P)$ ,  $O(^1D)$ ,  $O_2(a^1\Delta)$  and  $O_2(b^1\Sigma)$  produced by ionization under disturbed conditions is taken to be: 0.64, 0.16, 0.14, 0.06, 0.45, 0.61, 1.28, 0.10, 0.24 and 0.05 particles per ion pair, respectively. This distribution closely follows that of Gilmore,<sup>2,3</sup> except that  $N_2(A^3\Sigma)$  is not carried,  $[O_2(^1\Delta)]$  is taken as 0.24 and  $[O]$  is 1.28. Cases for daytime and nighttime conditions are reported; the calculations correspond to about a three hour interval centered around noon and midnight. Appropriate neutral densities have been outlined elsewhere.<sup>4</sup> The program coding and fixed input parameters have also been discussed previously.

It is the purpose of this report to: (1) display selected computed results as a function of time and ionization conditions, (2) show the results of comparison studies of a very limited nature, and (3) report the computed variations of the equivalent rate coefficients (ERC's) as a function of time and ionization conditions. (A copy of these BENCHMARK-76 results may be obtained by writing the authors.)

<sup>1</sup>E. L. Lortie, M. D. Kregel and F. E. Niles, "AIRCHEM: A Computational Technique for Modeling the Chemistry of the Atmosphere," BRL Report No. 1913, August 1976. (AD# A030157)

<sup>2</sup>F. Gilmore as quoted by B. F. Myers and M. R. Schoonover, "Electron Energy Degradation in the Atmosphere: Consequent Species and Energy Densities, Electron Flux, and Radiation Spectra," DNA 3513T, 3 Jan 75, Table 6.

<sup>3</sup>J. M. Heimerl and F. E. Niles, "BENCHMARK-76: Model Computations for Disturbed Atmospheric Conditions I. Input Parameters," BRL Report No. 2022, October 1977. (AD #A050355)

<sup>4</sup>F. E. Niles and J. M. Heimerl, "Selected Neutral Species Profiles 0-100 km," BRL Memo Report 2767, July 1977. (AD# A042620)

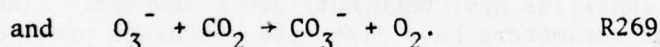
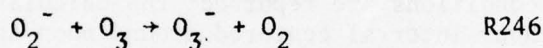
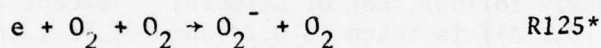
## RESULTS

### A. Selected Densities

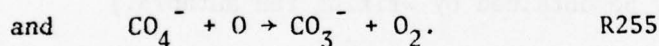
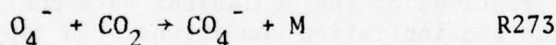
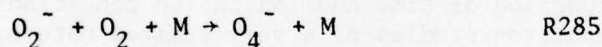
The daytime and nighttime electron density computed as a function of time after burst is shown for the six ionization conditions in Figures 1 and 2, respectively.

We might expect that the larger the disturbance, i.e., the larger the value of  $N_0$  for a given  $Q_0$ , the longer it would take for the electron density to return to its quiescent value. In Figure 1 curves 4 and 6 (also 2 and 3) at the latest times ( $t \geq 10^3$  s) show that the computed value of the electron density,  $[e]$ , for curve 4 (2) falls below that for curve 6 (3). To examine why our expectations are not borne out by these computations, let us focus attention on curves 4 and 6 of Figure 1.

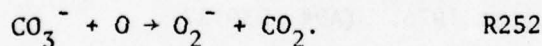
For both of these curves the main charge flow is found to be  $Q \rightarrow e \rightarrow O_2^- \rightarrow CO_3^-$ . The major reactions are



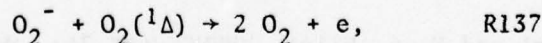
A secondary path exists; to wit,



In any event the charge at this point in the sequence resides upon the  $CO_3^-$  ion. The major loss process for this ion is found to be the reaction

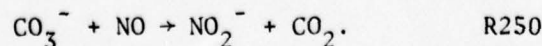


which simply cycles charge back to the  $O_2^-$  ion. The major loss of process for the  $O_2^-$  ion in both cases is the reaction



whose product is an electron and the entire cycle  $e \rightleftharpoons O_2^- \rightleftharpoons CO_3^-$  begins again.

For curve 4 there exists an important secondary loss process for the  $CO_3^-$  ion; namely, the reaction,



\* Read as reaction 125, see Appendix for complete reaction listing.

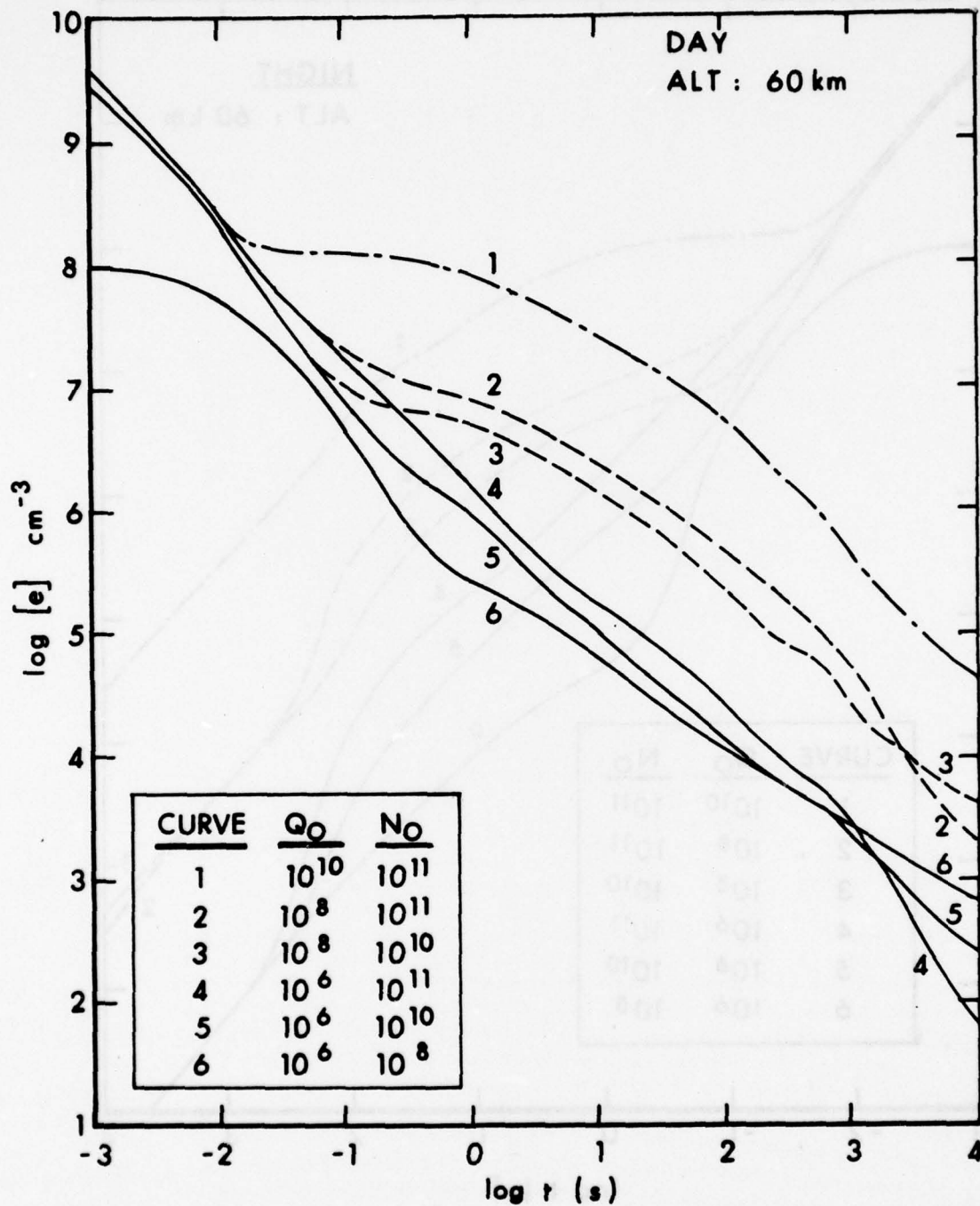


Figure 1. Logarithm of the computed daytime electron density at 60 km as a function of the logarithm of time for six different excitation conditions.  $Q_0$  is the delayed ionization parameter in ion-pairs  $\text{cm}^{-3}\text{s}^{-1}$  and  $N_0$  the prompt ionization parameter in  $\text{cm}^{-3}$ .

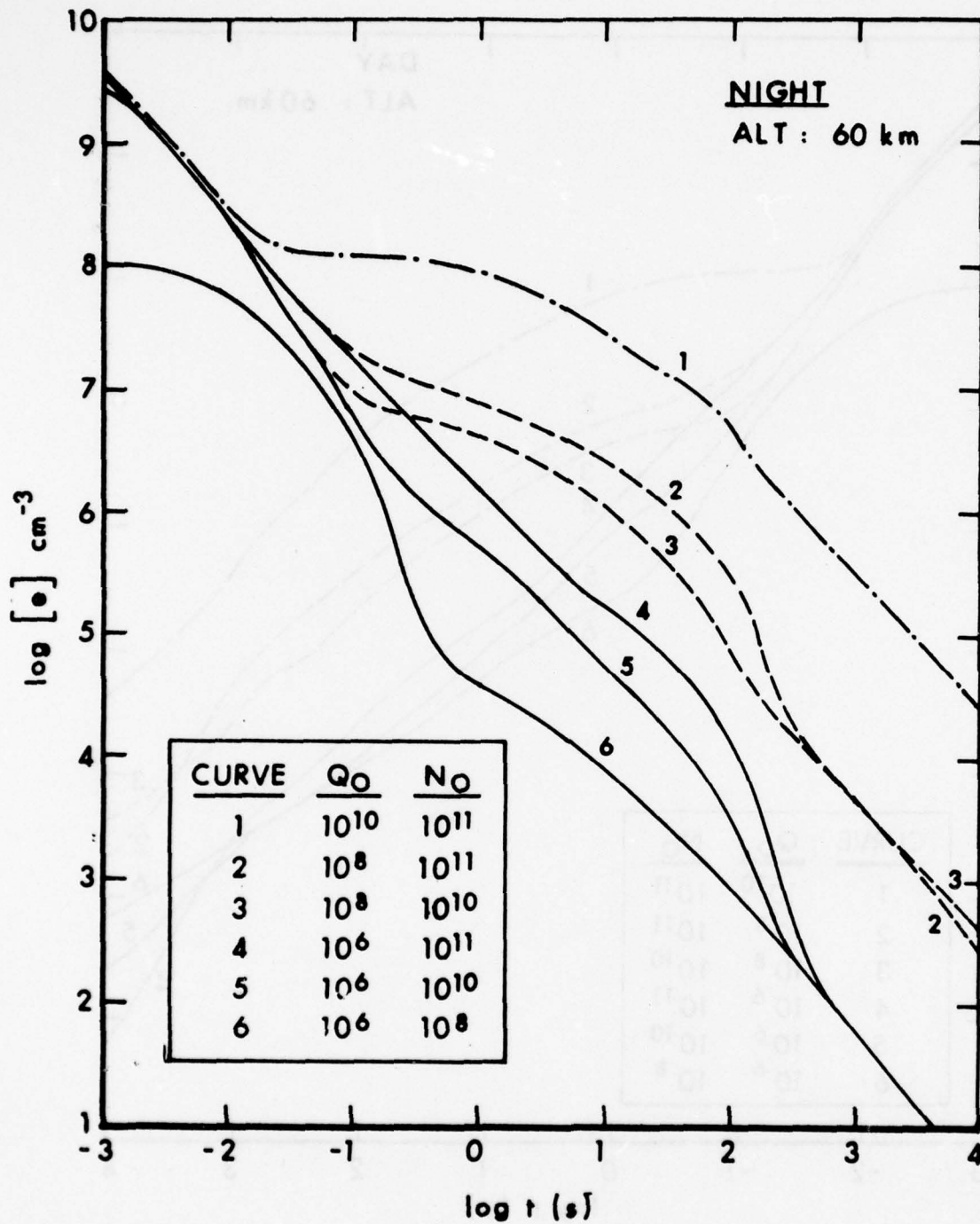
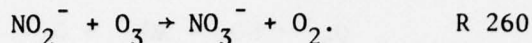


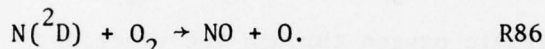
Figure 2. Same as Figure 1, except for nighttime conditions.

This reaction allows about 10% of the charge to flow to the  $\text{NO}_2^-$  ion which reacts rapidly to form the  $\text{NO}_3^-$  ion by the reaction



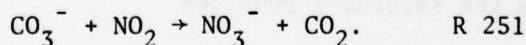
By contrast, reaction 250 for the conditions of curve 6 allows only about 0.1% of the charge to flow to the  $\text{NO}_3^-$  ion. It is the relative importance of the  $\text{CO}_3^-$  ion loss via reaction 250 that accounts for the calculated difference in the late time electron densities. For case 4 the charge that flows to the  $\text{NO}_3^-$  ion tends to remain bound to it. (The electron affinity of the  $\text{NO}_3^-$  ion ( $\text{EA} = 3.9 \text{ eV}$ )<sup>5</sup> is greater than that of the  $\text{O}_2^-$  ion ( $0.440 \text{ eV}$ )<sup>6</sup> or the  $\text{CO}_3^-$  ion ( $\text{EA} = 2.69 \text{ eV}$ )<sup>7</sup>.) This process tends to deplete the number density of free electrons. For curve 6, the path forming the  $\text{NO}_3^-$  ion is about a hundred times less effective than for curve 4 and the number density of free electrons tends to be maintained through the recycling process.

To find why reaction 250 is so pivotal a reaction the values of  $[\text{NO}]$  are examined at late times. It is found that the value of  $[\text{NO}]$  for curve 4 is about one hundred times larger than for curve 6. The reason for this lies in the formation of the  $\text{NO}$  molecule at the earliest times by the reaction



The value of  $[\text{N}(^2\text{D})]$ , hence the value of  $[\text{NO}]$  through reaction 86, is determined in large part by the value of the prompt ionization parameter,  $N_0$ . To summarize we find that for the same value of  $Q$ , the greater the value of  $N_0$ , the larger the value of  $[\text{NO}]$ , the larger the value of  $[\text{NO}_3^-]$ , the smaller the value of  $[e]$ . Similar arguments apply for curves 2 and 3 of Figure 1.

Figure 2 explicitly shows a similar phenomenon at the latest times for curves 2 and 3. Curves 4 and 6 also cross as in Figure 1 but their values are so similar to case 5 that they are indistinguishable on this scale. Arguments similar to the daytime case apply here, except that the details of the reactions change. As before, the main charge flow is given by  $Q \rightarrow e \rightarrow \text{O}_2 \rightarrow \text{CO}_3^-$  by reactions 125, 246 and 269. But here the major loss for the  $\text{CO}_3^-$  ion at late times at night is given by

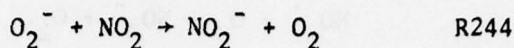


<sup>5</sup>See for example E. E. Ferguson, D. B. Dunkin and F. C. Fehsenfeld, "Reactions of  $\text{NO}_2^-$  and  $\text{NO}_3^-$  with  $\text{HCl}$  and  $\text{HBr}$ ," J. Chem. Phys. **57**, 1459-1463, 1972.

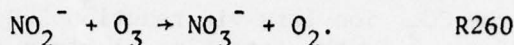
<sup>6</sup>R. J. Celotta, R. A. Bennett, J. L. Hall, M. W. Siegel and J. Levine, "Molecular Photodetachment Spectrometry. II. The Electron Affinity of  $\text{O}_2$  and the Structure of  $\text{O}_2^-$ ," Phys. Rev. **A6**, 631-642, 1972.

<sup>7</sup>S. P. Hong, S. B. Woo and E. M. Helmy, "Photodetachment of Thermally Relaxed  $\text{CO}_3^-$ ," Phys. Rev. **A15**, 1563-1569, 1977.

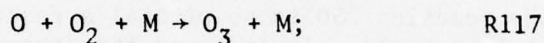
The  $\text{NO}_3^-$  ion formation is aided among other reactions by the secondary reactions



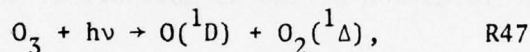
followed by



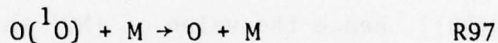
There are two differences for nighttime conditions. 1) The  $\text{NO}_2$  molecule rather than the NO molecule determines the charge flow to the  $\text{NO}_3^-$  ion and 2) the recycling of charge is not important at late times. This last difference comes about because reaction 252 is not an important loss process for  $\text{CO}_3^-$  at night. The fundamental reason for this lies in the fact that the value of  $[\text{O}]$  falls markedly at late times at night relative to the daytime case. Atomic oxygen is converted to ozone by the reaction



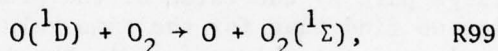
but the dominant daytime loss process for ozone, the reaction



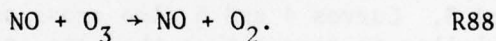
which returns atomic oxygen through the reactions



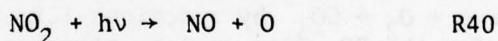
and



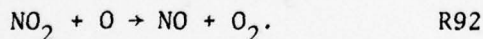
is unavailable at night. A similar photon reaction explains the NO/ $\text{NO}_2$  difference. To wit, at late times the primary source of the  $\text{NO}_2$  molecule is the reaction



In daytime the primary loss process for the  $\text{NO}_2$  molecule is the reaction



with aid from the secondary reaction



Again, at night when no photons are available reaction 40 is not significant. Reaction 92 does not compensate for the loss because as we have alluded to above the atomic oxygen density also falls at late times at night with the result that the  $[\text{NO}_2]$  builds.

The dominant electron depopulating process at late times for both day and night conditions (Figures 1 and 2) is three body attachment. At night the dominant electron production mechanism at late times is the delayed ionization source term whose value is given by  $Q$  (see equation 1). Thus at the later times the electron densities tend to track  $Q$ . For daytime conditions the recycling of charge, as discussed above, may permit the rates of other reactions to compete with the source rate with the result that the daytime electron densities need not, in general, track  $Q$ .

Figures 3 and 4 show the sum of the negative ions (exclusive of electrons) computed as a function of time. Conditions correspond to those in Figures 1 and 2, respectively. Figures 5 and 6 show the corresponding plots for the sum of the positive ions.

For times less than  $10^{-2}$  seconds, the electron and positive ion curves (Figures 1, 2, 5 and 6) tend to group according to the prompt ionization parameter,  $N_0$ . For times greater than  $10^{-1}$  seconds they tend to group according to the delayed ionization parameter,  $Q_0$ .

Some of the curves cease abruptly in these (and other) figures because computations are automatically halted whenever the electron density falls below  $10 \text{ cm}^{-3}$ , the assumed quiescent background electron density.

#### B. Comparison

Figures 7 and 8 show the electron density computed as a function of time at 60 km altitude for both the present results (BRL-76) and the DCHEM results of Scheibe<sup>8</sup> for daytime and nighttime, respectively. In spite of the fact that different sets of chemical reactions<sup>9</sup> and integration schemes were employed, the agreement is very good to excellent. Both day and night comparisons have also been made and reported<sup>10</sup> for the fixed ionization conditions  $Q_0 = 10^8 \text{ ion-pairs-cm}^{-3}\text{-s}^{-1}$  and  $N_0 = 10^{11} \text{ cm}^{-3}$ . These comparisons indicate a basic overall agreement between Scheibe's results and our own for the computation of the electron density at 60 km as a function of Day/Night conditions, of excitation and of time.

<sup>8</sup>W. S. Knapp, "A Simplified D-Region Chemistry Model for Nuclear Environments," DNA 2850T, April 72; also M. Scheibe, private communication, 1976.

<sup>9</sup>For example, the BENCHMARK-76 reaction set includes neutral odd-hydrogen reactions; Scheibe's set does not.

<sup>10</sup>J. M. Heimerl and F. E. Niles, "BENCHMARK-76: Model Computations for Disturbed Atmospheric Conditions II. Results for the Stratosphere and Mesosphere," BRL Technical Report ARBRL-TR-02050, March 1978.

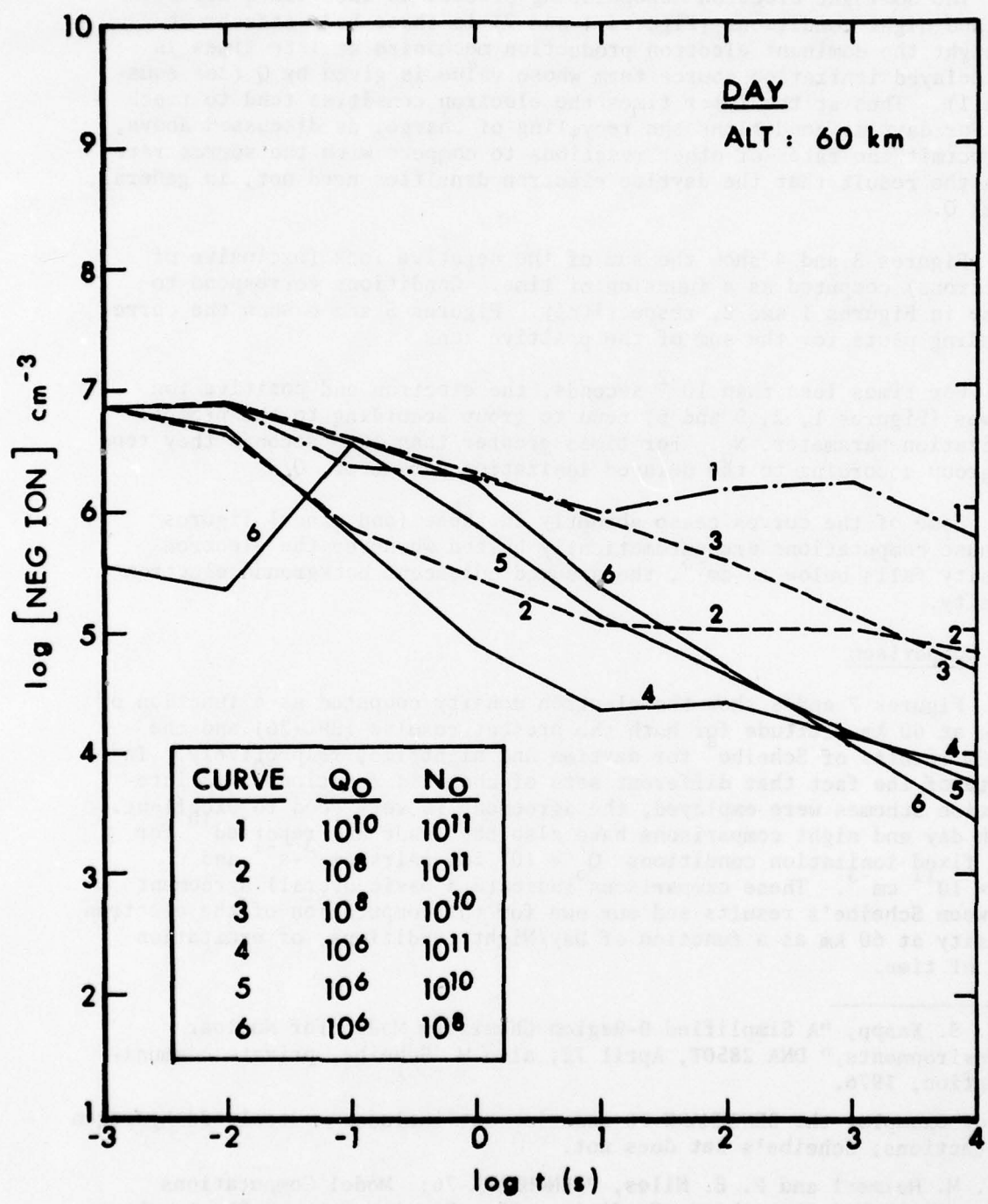


Figure 3. Logarithm of the daytime total negative ion density 60 km as a function of the logarithm of time for six different ionization conditions.

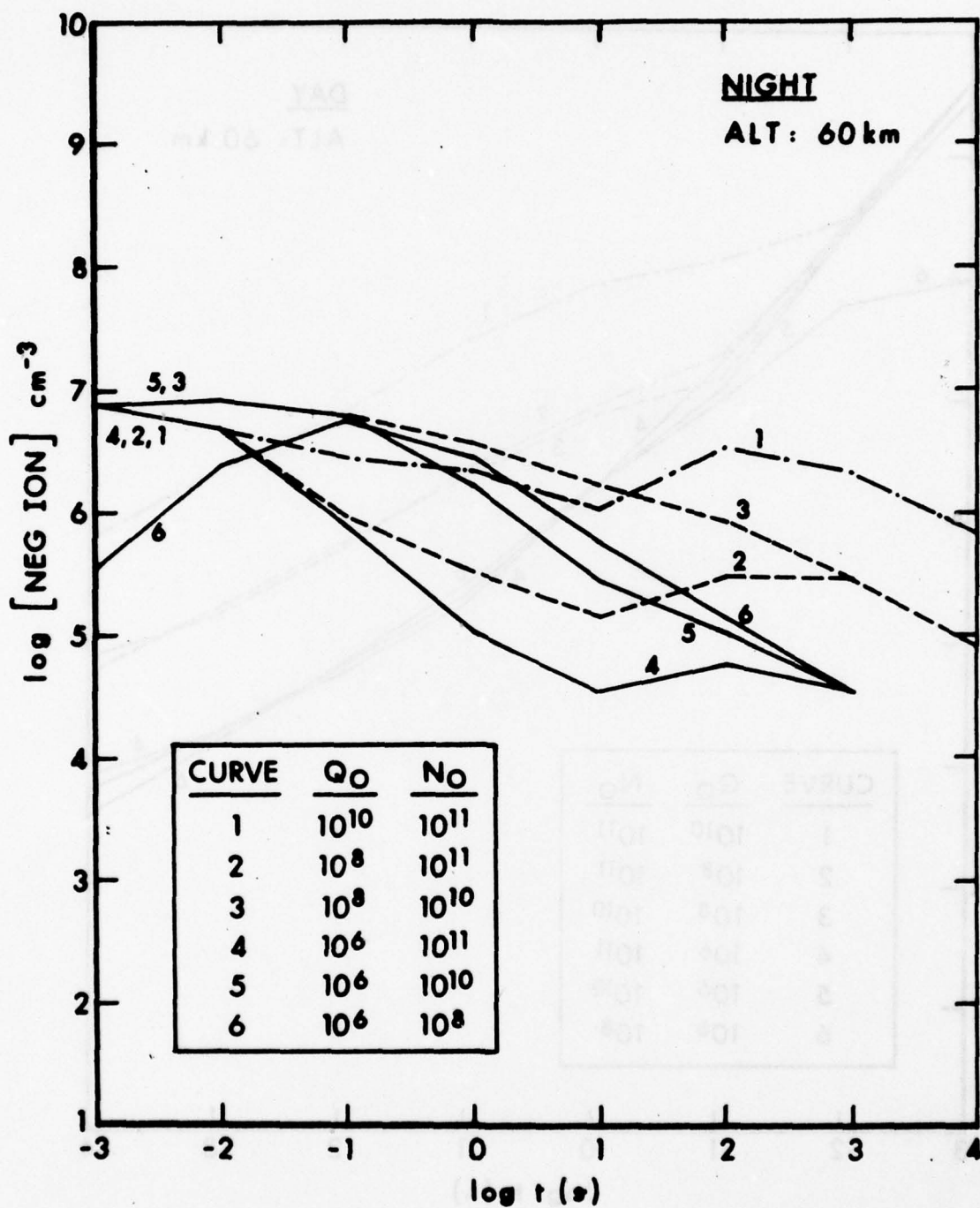


Figure 4. Same as Figure 3, except for nighttime conditions.

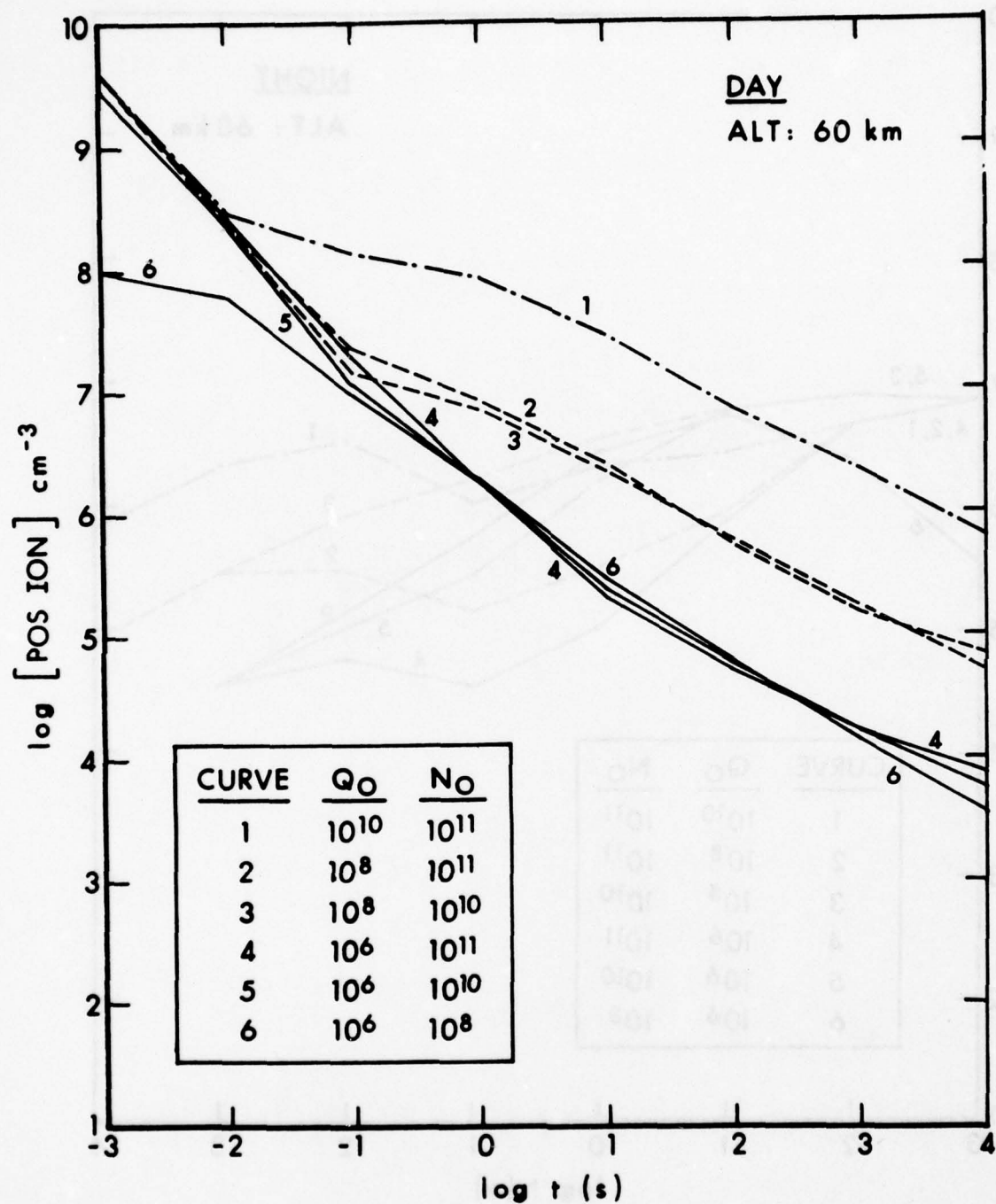


Figure 5. Logarithm of the daytime total positive ion density at 60 km as a function of the logarithm of time for six ionization conditions.

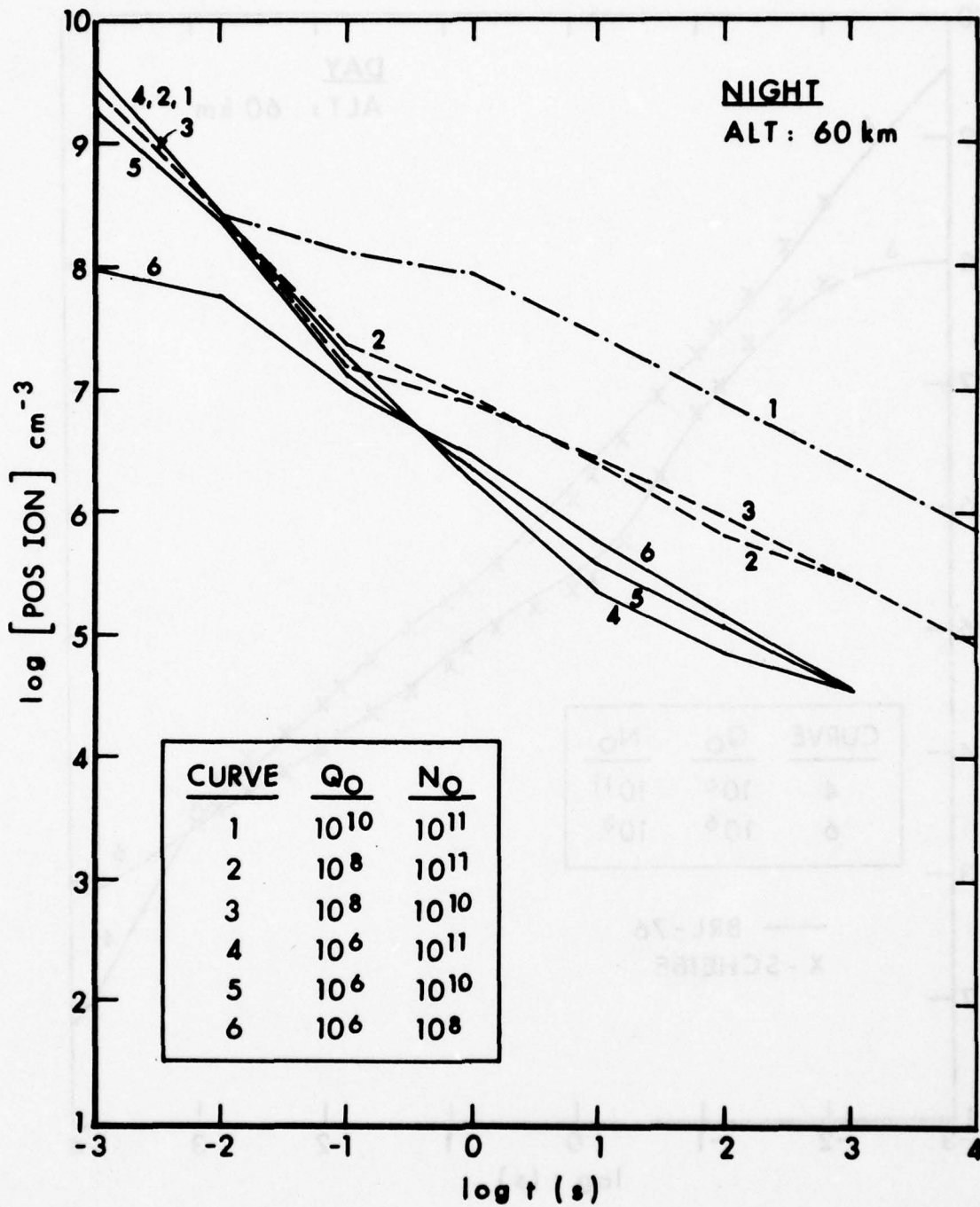


Figure 6. Same as Figure 5, except for nighttime conditions.

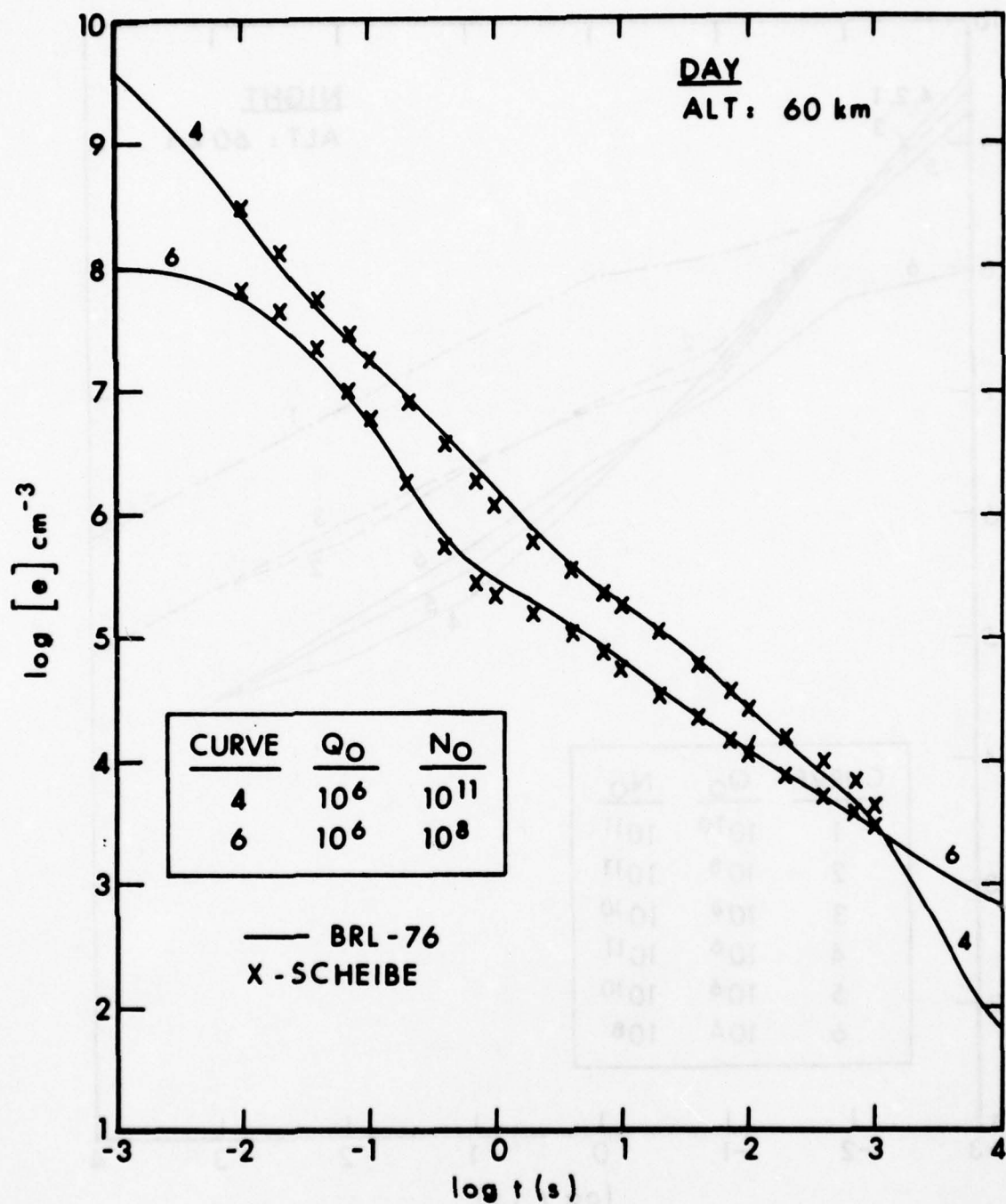


Figure 7. For two excitation conditions at 60 km the logarithm of the daytime electron density as computed by BRL's BENCHMARK-76 code (—) and Schiebe's DAIRCHEM code (X) vs. the logarithm of time.

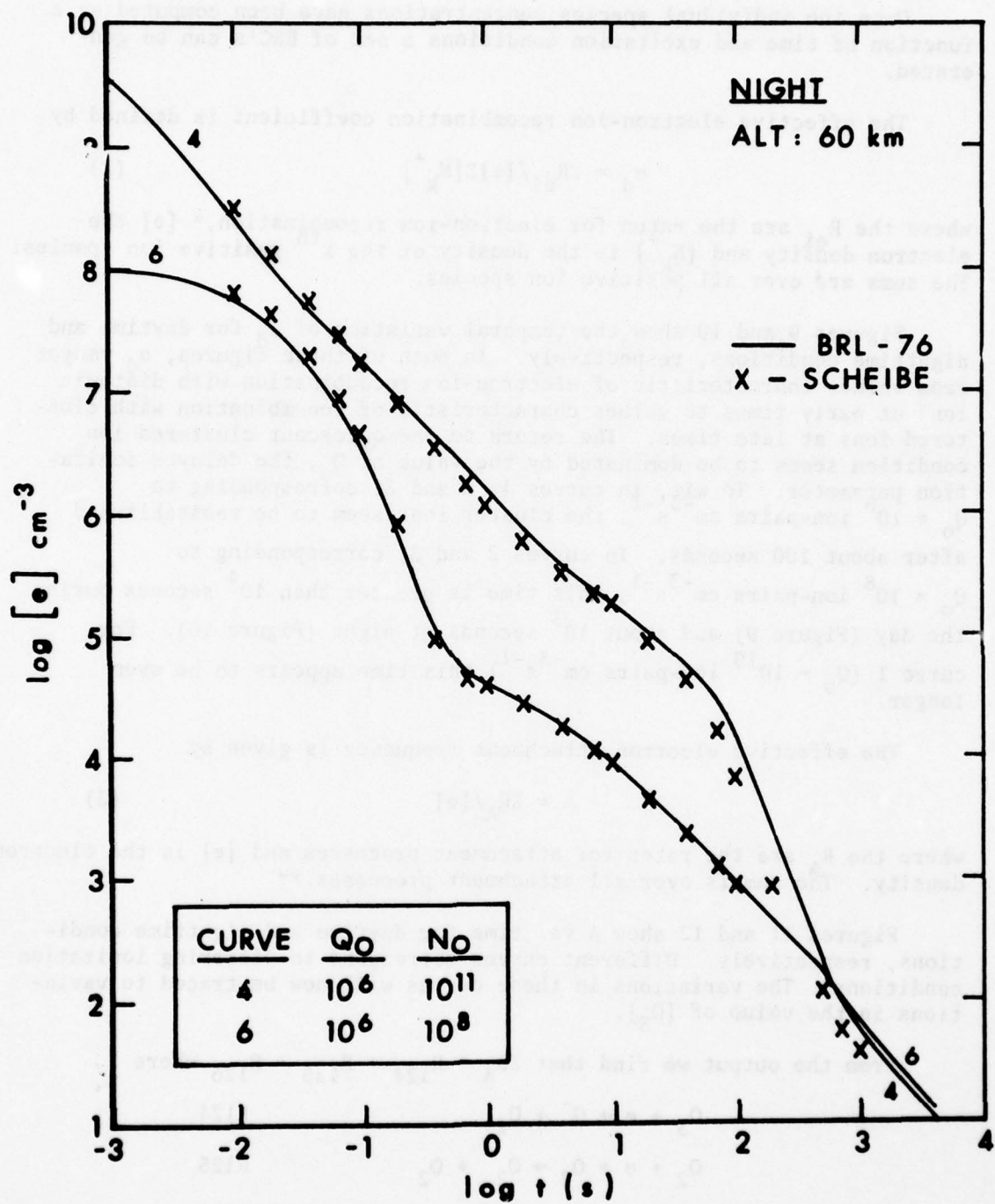


Figure 8. Same as Figure 7, except for nighttime conditions.

### C. Equivalent Rate Coefficients (ERC's)

Once the individual species concentrations have been computed as a function of time and excitation conditions a set of ERC's can be generated.

The effective electron-ion recombination coefficient is defined by

$$\alpha_d = \Sigma R_{ei} / [e] \Sigma [N_k^+] \quad (2)$$

where the  $R_{ei}$  are the rates for electron-ion recombination,\*  $[e]$  the electron density and  $[N_k^+]$  is the density of the  $k^{\text{th}}$  positive ion species. The sums are over all positive ion species.

Figures 9 and 10 show the temporal variation of  $\alpha_d$  for daytime and nighttime conditions, respectively. In both of these figures,  $\alpha_d$  ranges from values characteristic of electron-ion recombination with diatomic ions at early times to values characteristic of recombination with clustered ions at late times. The return to the quiescent clustered ion condition seems to be dominated by the value of  $Q_0$ , the delayed ionization parameter. To wit, in curves 4, 5 and 6, corresponding to  $Q_0 = 10^6$  ion-pairs  $\text{cm}^{-3}\text{s}^{-1}$ , the cluster ions seem to be reestablished after about 100 seconds. In curves 2 and 3, corresponding to  $Q_0 = 10^8$  ion-pairs  $\text{cm}^{-3}\text{s}^{-1}$ , this time is greater than  $10^4$  seconds during the day (Figure 9) and about  $10^3$  seconds at night (Figure 10). For curve 1 ( $Q_0 = 10^{10}$  ion-pairs  $\text{cm}^{-3}\text{s}^{-1}$ ) this time appears to be even longer.

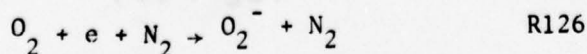
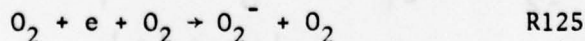
The effective electron attachment frequency is given by

$$A = \Sigma R_A / [e] \quad (3)$$

where the  $R_A$  are the rates for attachment processes and  $[e]$  is the electron density. The sum is over all attachment processes.\*\*

Figures 11 and 12 show  $A$  vs. time for daytime and nighttime conditions, respectively. Different curves correspond to differing ionization conditions. The variations in these curves will now be traced to variations in the value of  $[O_3]$ .

From the output we find that  $\Sigma R_A \approx R_{124} + R_{125} + R_{126}$  where



\* Reactions 138-162, inclusive (see Appendix)

\*\* Reactions 122-126, inclusive (see Appendix)

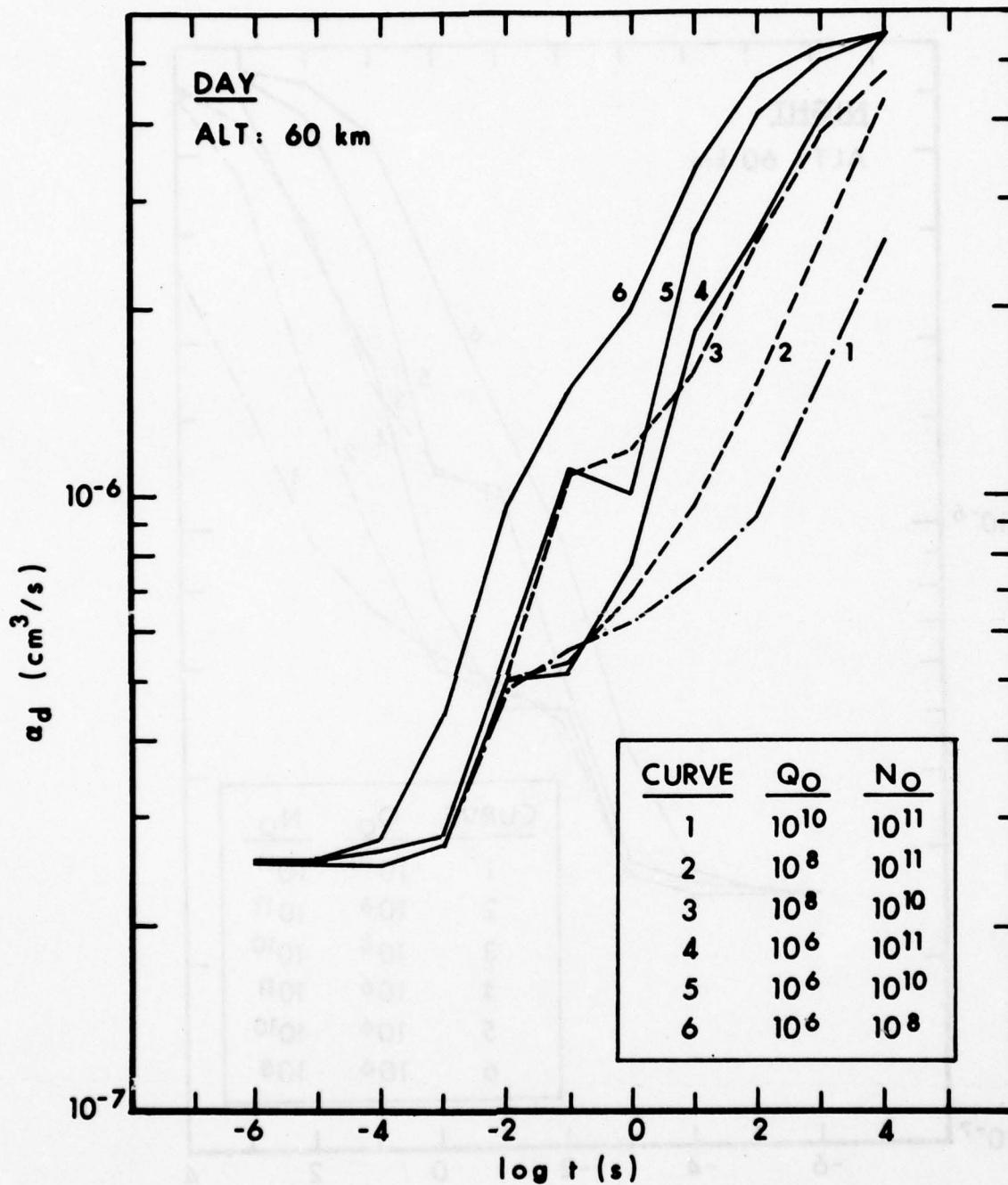


Figure 9. Logarithm of the computed daytime effective electron-ion recombination coefficient,  $\alpha_d$ , at 60 km as a function of the logarithm of time for six ionization conditions.

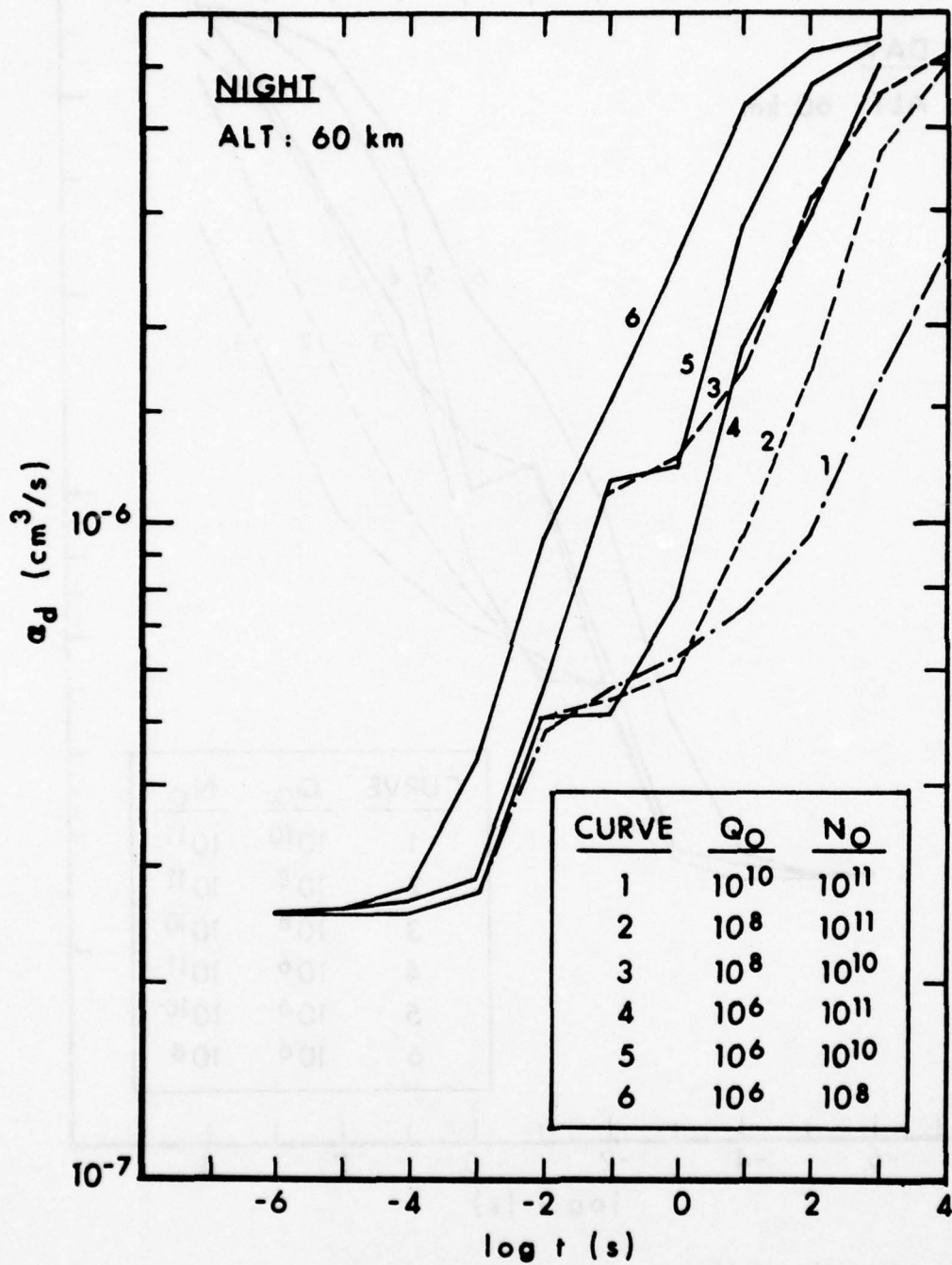


Figure 10. Same as Figure 9, except for nighttime conditions.

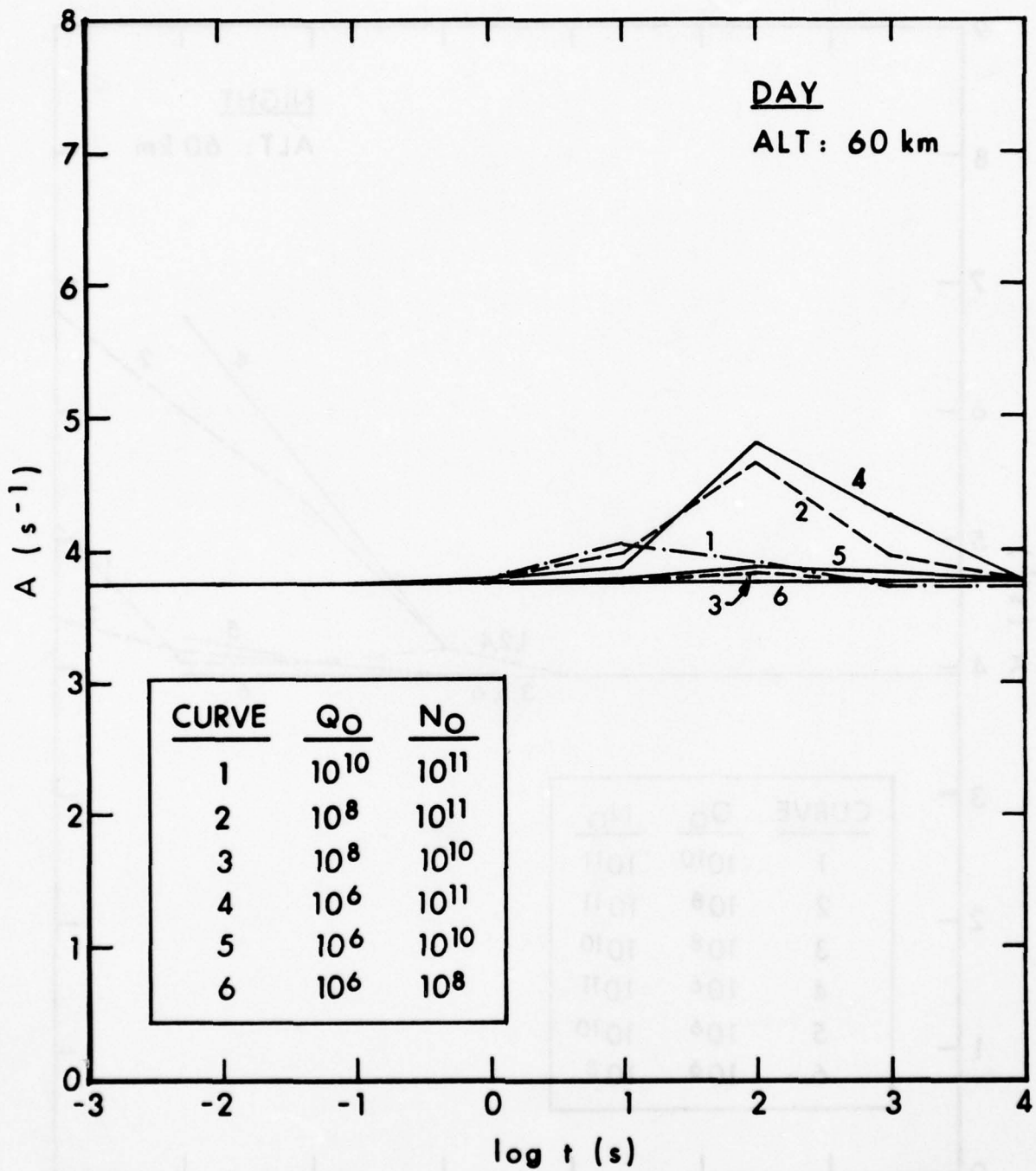


Figure 11. Logarithm of the computed daytime effective attachment frequency,  $A$ , at 60 km as a function of the logarithm of time for six ionization conditions.

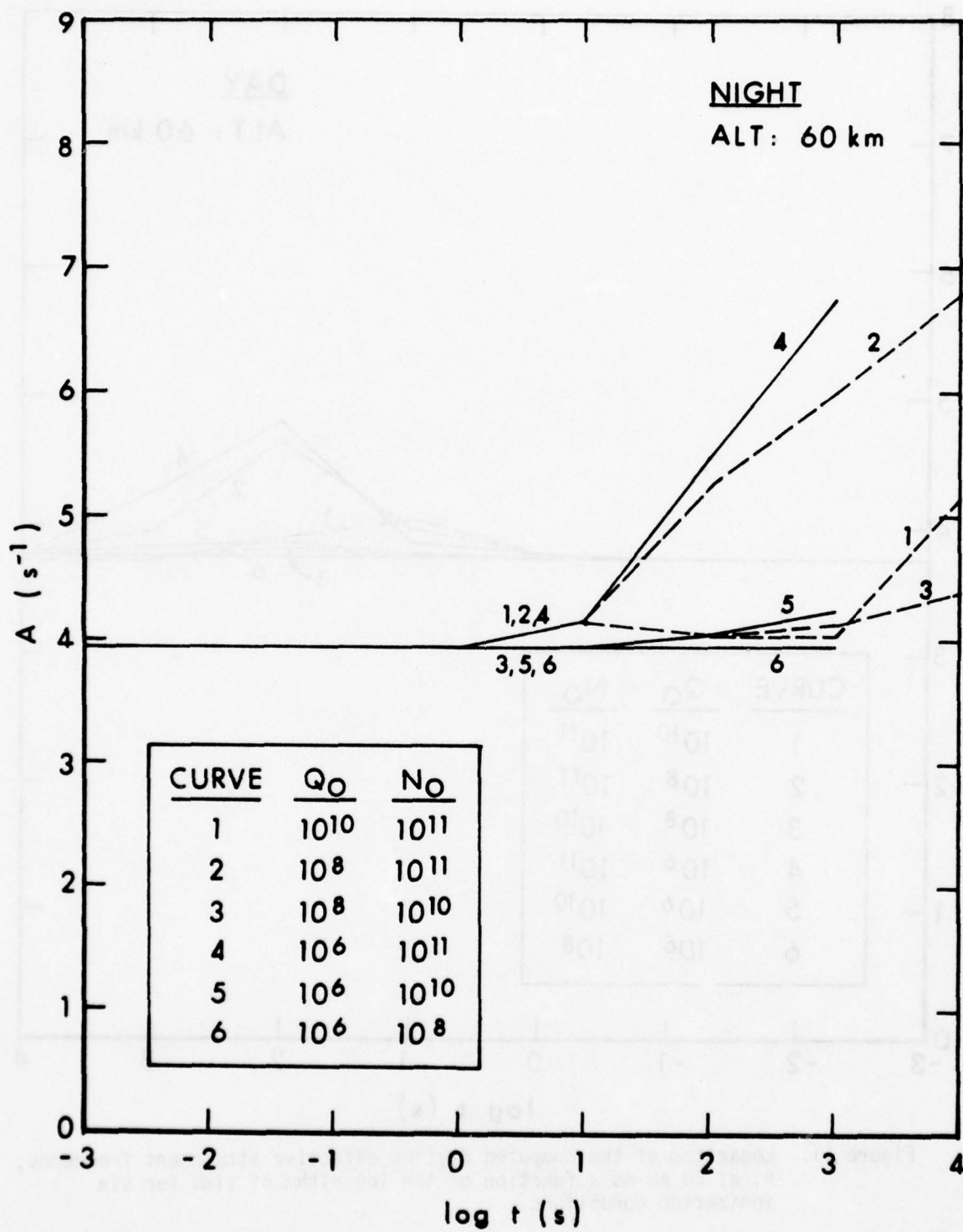


Figure 12. Same as Figure 11, except for nighttime conditions.

Substituting into equation (3) we find that

$$A \approx C(1 + B) \quad (4)$$

where

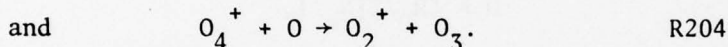
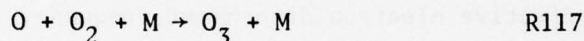
$$C = k_{125}[O_2]^2 + k_{126}[O_2][N_2] \quad (5)$$

and

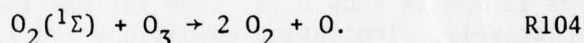
$$B = k_{124}[O_3]/C. \quad (6)$$

Since C in Equation (5) is constant to several decimal places and since  $k_{124}$  in Equation (6) is held fixed, the changes in the value of A in Equation (4) must reflect changes in the ozone concentration.

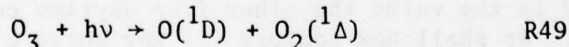
For the daytime case, Figure 11, let us consider curve 4 since it has the largest excursion. Figure 11 shows three easily determined time domains. For  $10^{-3} \leq t \leq 10^{-1}$  s A is observed to be constant. It is found that B of Equation (6) is 0.01 in this time period. [B of Equation (6) is simply a measure of the relative importance of  $R_{124}/(R_{125} + R_{126})$ .] Thus Equations (4) and (5) show that at early times  $A \approx C$ . The reason that the value of  $[O_3]$  remains constant over this interval lies in the near balance between the production and loss rates of ozone. The major reactions populating ozone are



Reaction 204 is found to be an important source of  $O_3$  up to and including  $t = 10^{-2}$  s. The major reaction depopulating ozone over this time interval is

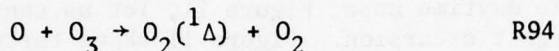
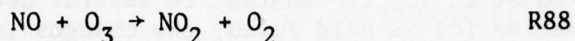


The overall effect of reactions 117 and 104 is to convert  $O_2(^1\Sigma)$  to  $O_2$ . Eventually  $[O_2(^1\Sigma)]$  is depleted and for times greater than  $10^{-1}$  s the value of  $[(O_2(^1\Sigma))]$  falls to such an extent that the production rate (now due almost exclusively to Reaction 117) exceeds the loss rate with the result that the ozone concentration rises. By  $10^2$  seconds the ozone concentration has risen to such an extent that the rate of  $O_3$  loss by the reaction



tends to balance the  $O_3$  production rate. For times greater than  $10^3$  s the value of  $[O_3]$  tracks the value of  $[O]$  (in fact their densities are about equal) and since the value of the atomic oxygen begins to fall, the value of the ozone density does also.

At night only two time domains are observed in Figure 12. For times less than  $10^0$  s the daytime arguments apply for A constant. For times greater than  $10^0$  seconds the loss rates which are due to



and Reaction (104) fall relative to the production by Reaction (117) and again the rise in the value of  $[\text{O}_3]$  is reflected by an increase in the value of A in Figure 12.<sup>3</sup> The ozone density,  $[\text{O}_3]$ , will not rise indefinitely. In fact at  $10^3$  s the major loss rate, which is due to Reaction 88, greatly exceeds the production rate to 117 thus we would anticipate the value of  $[\text{O}_3]$  (hence the value of A) to fall as in the daytime case but at times later than those graphed in Figure 12.

The effective electron detachment frequency is defined by

$$D = \Sigma R_D / \Sigma [N_k^-], \quad (7)$$

where the  $R_D$  are the rates for individual detachment processes\* and  $[N_k^-]$  is the  $k^{\text{th}}$  negative ion density. The sums are over all detachment rates and all negative ion densities, respectively.

Figures 13 and 14 show D vs. time for daytime and nighttime conditions, respectively. Ionization conditions are listed nearby their corresponding curves. The most notable feature in both Figures 13 and 14 is the apparent grouping of the curves. There are three groups, the first composed of curves 1, 2 and 4; the second of curves 3 and 5 and the third of curve 6. From the key on these figures we find that they are grouped according to the prompt ionization parameter,  $N_0$ .

In Figure 13 curve 6 attains the approximate limit of  $10^0 \text{ s}^{-1}$  after  $10^0$  seconds. This limiting value is typical of daytime quiescent conditions and is the value the other five daytime curves should approach, but do not. We shall now address (1) why curve 6 attains its limiting value and (2) why the others do not attain a similar limit. To be specific we shall concentrate our attention on curve 4 as a contrast to curve 6.

It is found to a good approximation that

$$\Sigma R_D \approx R_{137} + R_{135} + R_{129},$$

\* Reactions 1-5 and 11 for photodetachment; 127-137 inclusive for two body collisional detachment. See Appendix for reaction list.

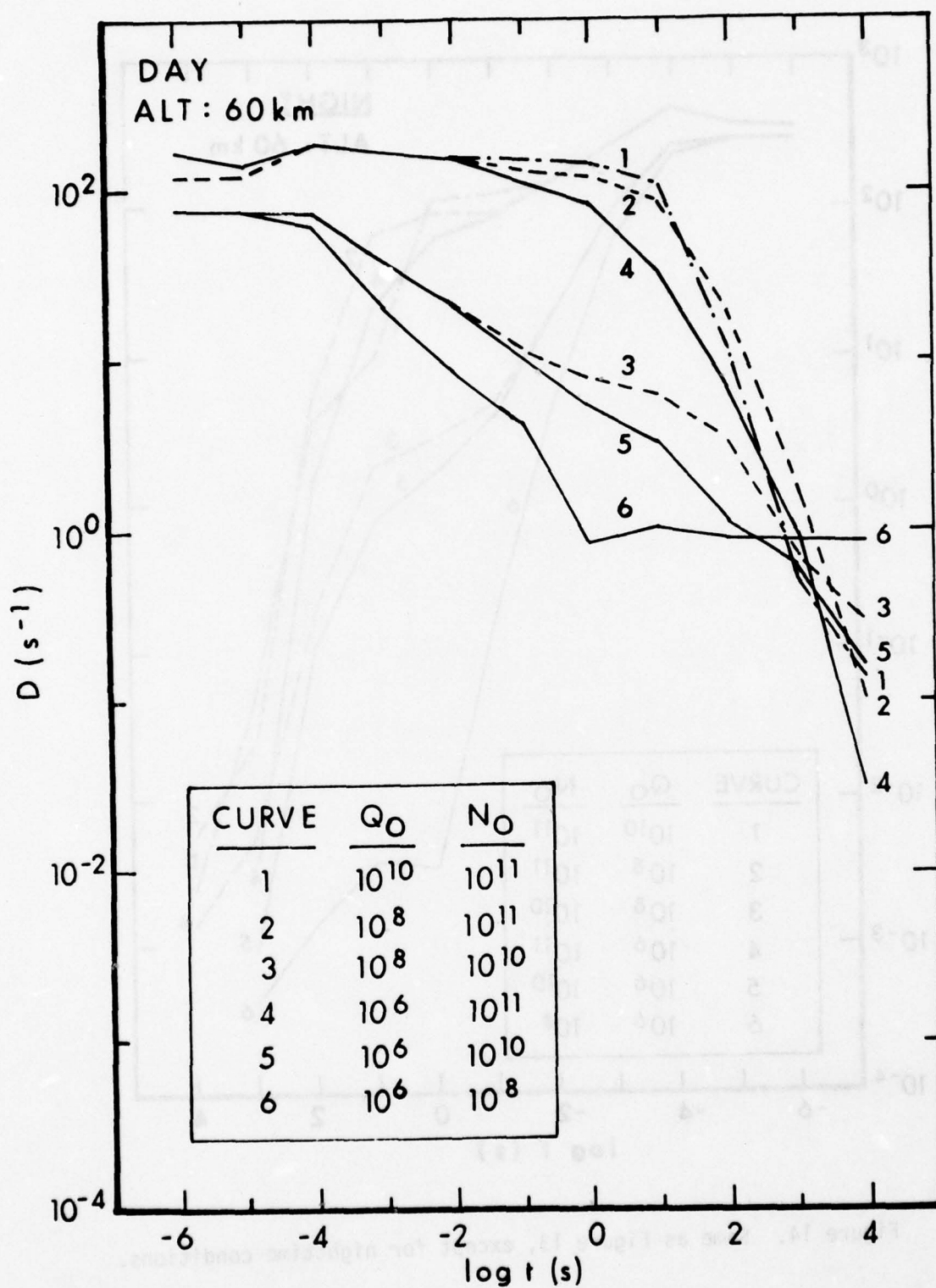


Figure 13. Logarithm of the computed daytime effective electron detachment frequency,  $D$ , at 60 km as a function of the logarithm of time for six ionization conditions.

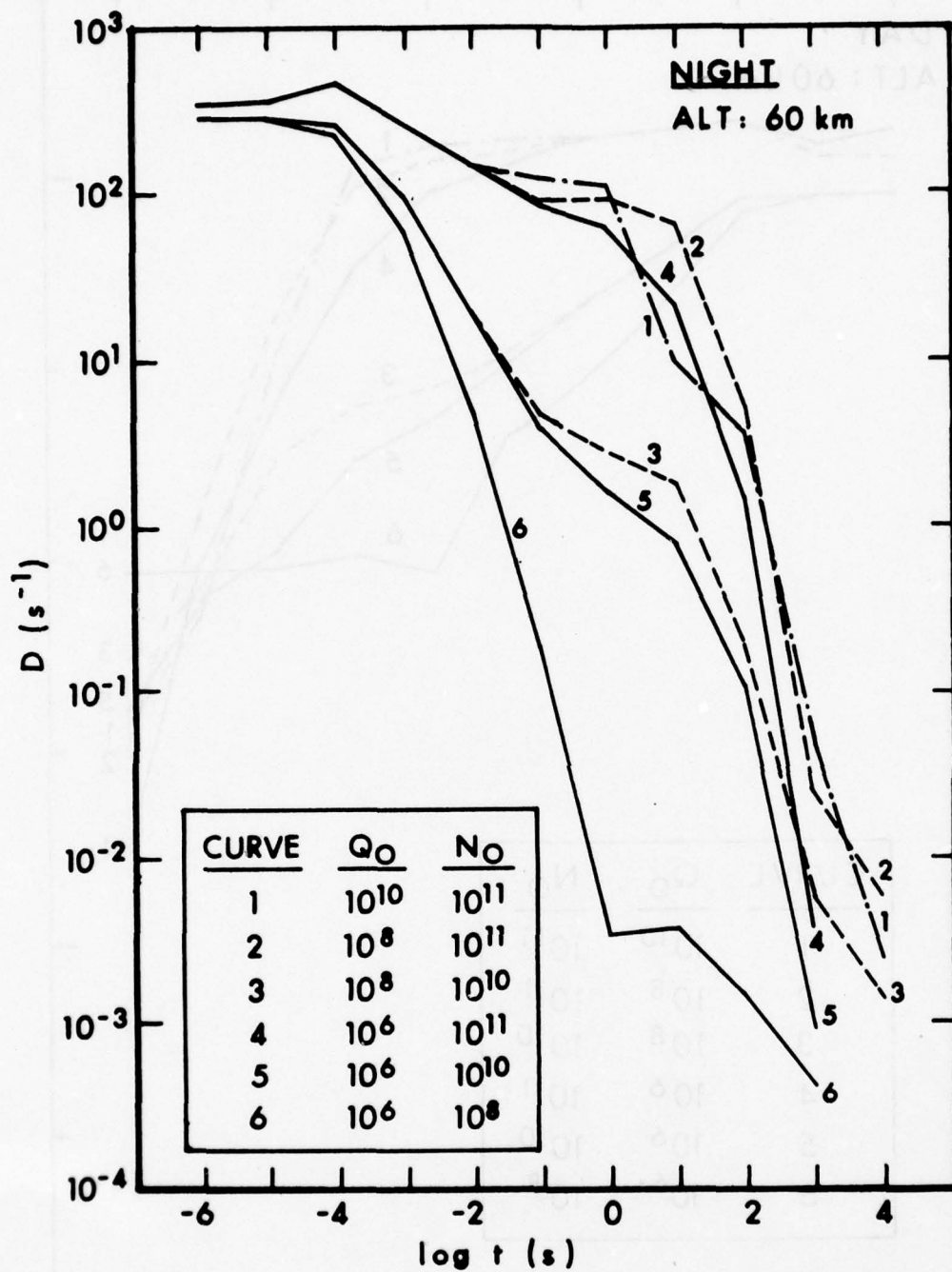


Figure 14. Same as Figure 13, except for nighttime conditions.

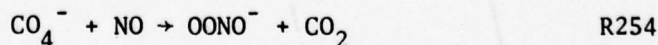
substituting this expression into Equation (7) we have

$$D \approx (k_{137}[O_2(^1\Delta)] + k_{135}[O]) ([O_2^-]/\Sigma[N_k^-]) + k_{129}[N_2][O^-]/\Sigma[N_k^-]. \quad (8)$$

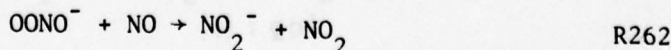
For case 6 we see from Figure 15 that for times greater than  $10^0$ s  $\Sigma[N_k^-] \approx [CO_3^-]$ . In addition  $[O_2^-]/[CO_3^-]$  and  $[O^-]/[CO_3^-]$  are approximately constant over this time interval (see Fig. 15). Since the value of  $[N_2]$  and the rate coefficients are constant the behavior of the  $O_2(^1\Delta)$  molecule and of the O atom needs to be examined. Over the interval  $10^1 \leq t \leq 10^4$ s, the value of  $[O_2(^1\Delta)]$  monotonically rises from  $1.5 \times 10^{10} \text{ cm}^{-3}$  to  $3.4 \times 10^{10} \text{ cm}^{-3}$ . There is no dramatic change in the value of  $[O]$  either. It first declines from  $1.4 \times 10^{10} \text{ cm}^{-3}$  to  $1.1 \times 10^{10} \text{ cm}^{-3}$ , then rises to  $1.3 \times 10^{10} \text{ cm}^{-3}$ . Since  $k_{137}$  and  $k_{135}$  are comparable ( $2 \times 10^{-10} \text{ cm}^3/\text{s}$  vs.  $1.5 \times 10^{-10} \text{ cm}^3/\text{s}$ , respectively) the variations in the values of  $[O_2(^1\Delta)]$  and  $[O]$  tend to offset each other. Thus for case 6 and for times greater than  $10^0$ s D is approximately constant.

On the other hand, Figure 16 shows for case 4 and for times greater than  $10^1$ s that  $\Sigma[N_k^-] \approx [NO_3^-]$ . In addition both  $[O_2^-]/[NO_3^-]$  and  $[O^-]/[NO_3^-]$  can be seen from the figure to be declining functions of time. The value of  $[O]$  monotonically declines from  $4.4 \times 10^{11} \text{ cm}^{-3}$  to  $1.0 \times 10^{10} \text{ cm}^{-3}$  ( $10^1 \leq t \leq 10^4$ s), while the value of  $[O_2(^1\Delta)]$  first rises from  $4.0 \times 10^{10} \text{ cm}^{-3}$  ( $t = 10^1$ s) to  $3.4 \times 10^{11} \text{ cm}^{-3}$  ( $t = 10^3$ s), then falls to  $2.7 \times 10^{10} \text{ cm}^{-3}$  ( $t = 10^4$ s). Since  $k_{137}$  and  $k_{135}$  are comparable, the declining value of  $[O]$  tends to offset the rising value of  $[O_2(^1\Delta)]$ . Thus D in Equation (8) will follow the ratio of the negative ion densities and the net result is that D for case 4 and for times greater than  $10^1$ s is a decreasing function of time. Cases 1, 2, 3 and 5 are similar to case 4.

One can ask why the late time dominant negative ion is  $NO_3^-$  in case 4 (and in other cases) but not in case 6. The answer to this is found to be in the production of the  $NO_3^-$  ion from either the  $CO_3^-$  or  $CO_4^-$  ions. The specific reactions are found to be



followed by



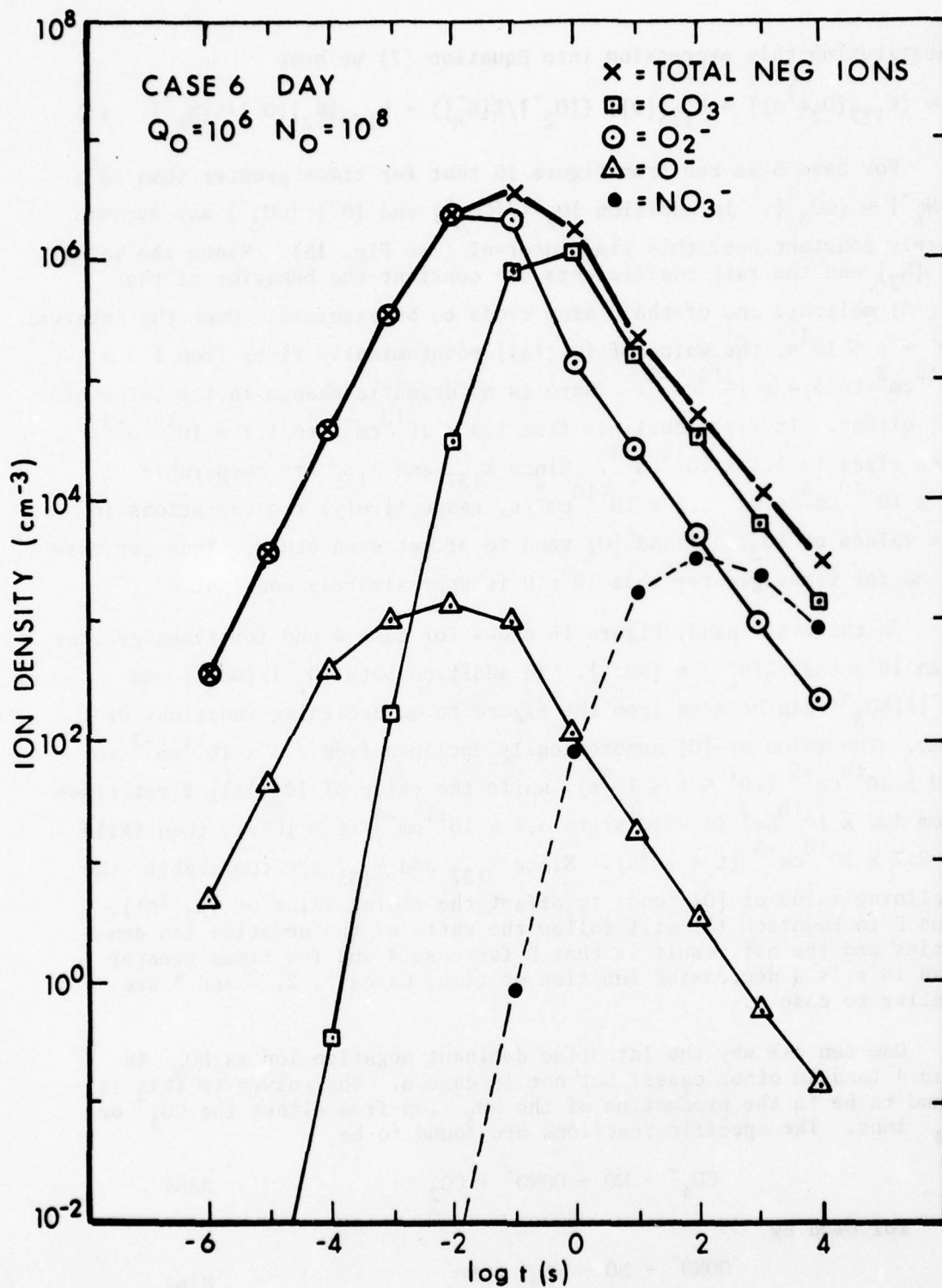


Figure 15. Histories of selected daytime negative ion densities at 60 km for the excitation conditions:  $Q_0 = 10^6$  ion-pairs  $\text{cm}^{-3}\text{s}^{-1}$  and  $N_0 = 10^8$   $\text{cm}^{-3}$  (Case 6). The  $\text{NO}_3^-$  ion density, dashed line, is shown for easy comparison with Case 4, Fig. 16.

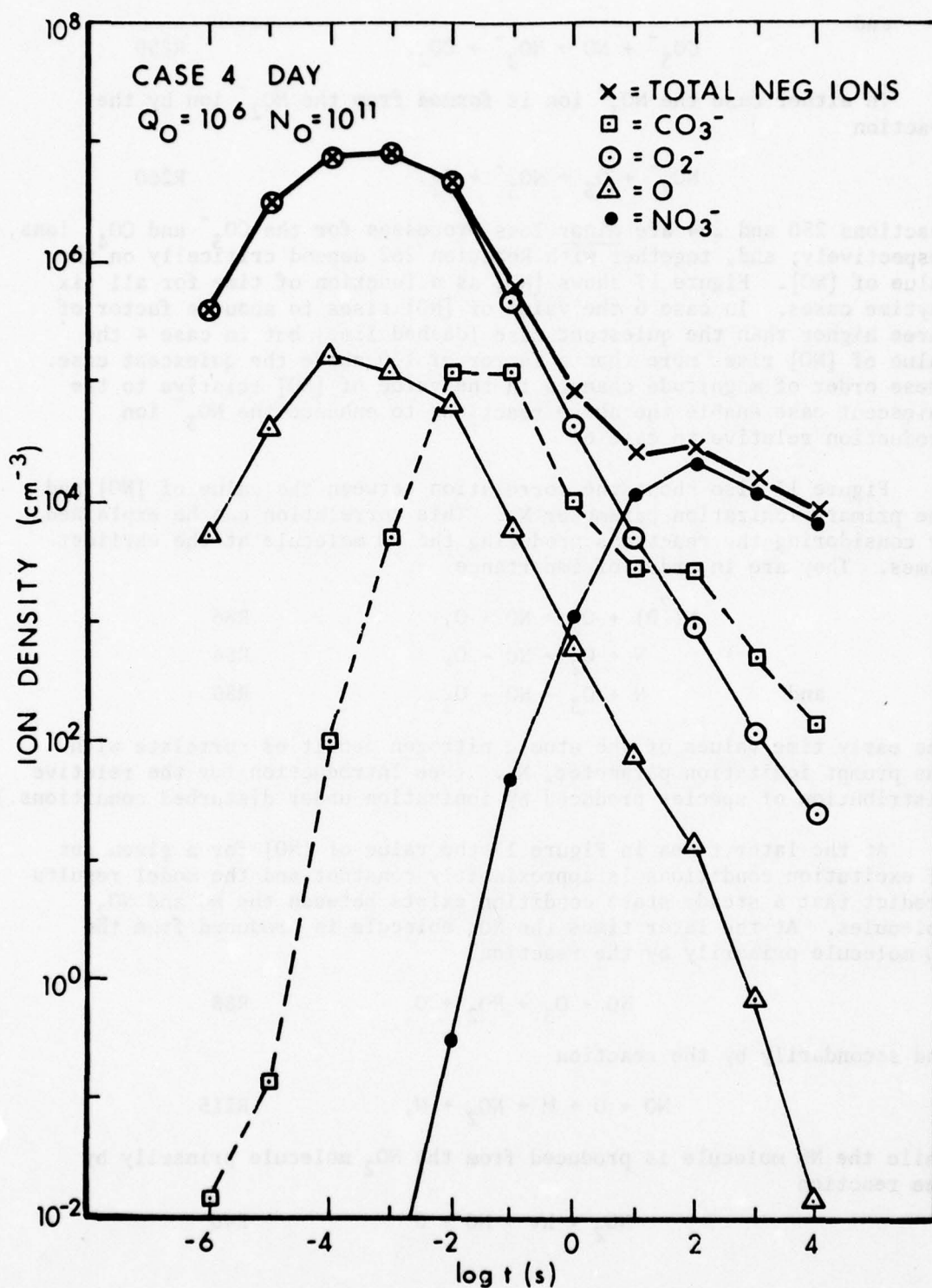
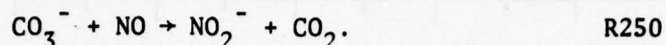
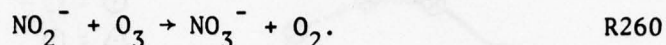


Figure 16. Histories of selected daytime negative ion densities at 60 km for the excitation conditions:  $Q_0 = 10^6$  ion-pairs  $\text{cm}^{-3}\text{s}^{-1}$  and  $N_0 = 10^{11} \text{ cm}^3$  (Case 4). The  $\text{CO}_3^-$  ion density, dashed line, is shown for easy comparison with Case 6, Fig. 15.

and

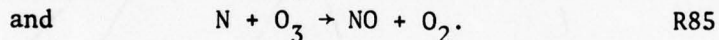
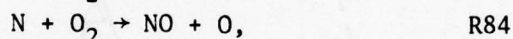
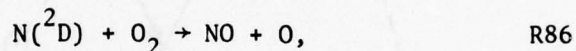


In either case the  $\text{NO}_3^-$  ion is formed from the  $\text{NO}_2^-$  ion by the reaction



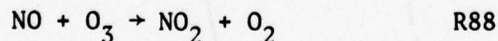
Reactions 250 and 254 are minor loss processes for the  $\text{CO}_3^-$  and  $\text{CO}_4^-$  ions, respectively; and, together with Reaction 262 depend critically on the value of  $[\text{NO}]$ . Figure 17 shows  $[\text{NO}]$  as a function of time for all six daytime cases. In case 6 the value of  $[\text{NO}]$  rises to about a factor of three higher than the quiescent case (dashed line) but in case 4 the value of  $[\text{NO}]$  rises more than a factor of 100 above the quiescent case. These order of magnitude changes in the value of  $[\text{NO}]$  relative to the quiescent case enable the above reactions to enhance the  $\text{NO}_3^-$  ion production relative to case 6.

Figure 17 also shows the correlation between the value of  $[\text{NO}]$  and the primary ionization parameter  $N_0$ . This correlation can be explained by considering the reactions producing the NO molecule at the earliest times. They are in order of importance

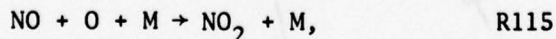


The early time values of the atomic nitrogen densities correlate with the prompt ionization parameter,  $N_0$ . (See Introduction for the relative distribution of species produced by ionization under disturbed conditions.)

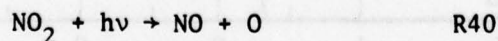
At the later times in Figure 17 the value of  $[\text{NO}]$  for a given set of excitation conditions is approximately constant and the model results predict that a steady state condition exists between the NO and  $\text{NO}_2$  molecules. At the later times the  $\text{NO}_2$  molecule is produced from the NO molecule primarily by the reaction



and secondarily by the reaction



while the NO molecule is produced from the  $\text{NO}_2$  molecule primarily by the reaction



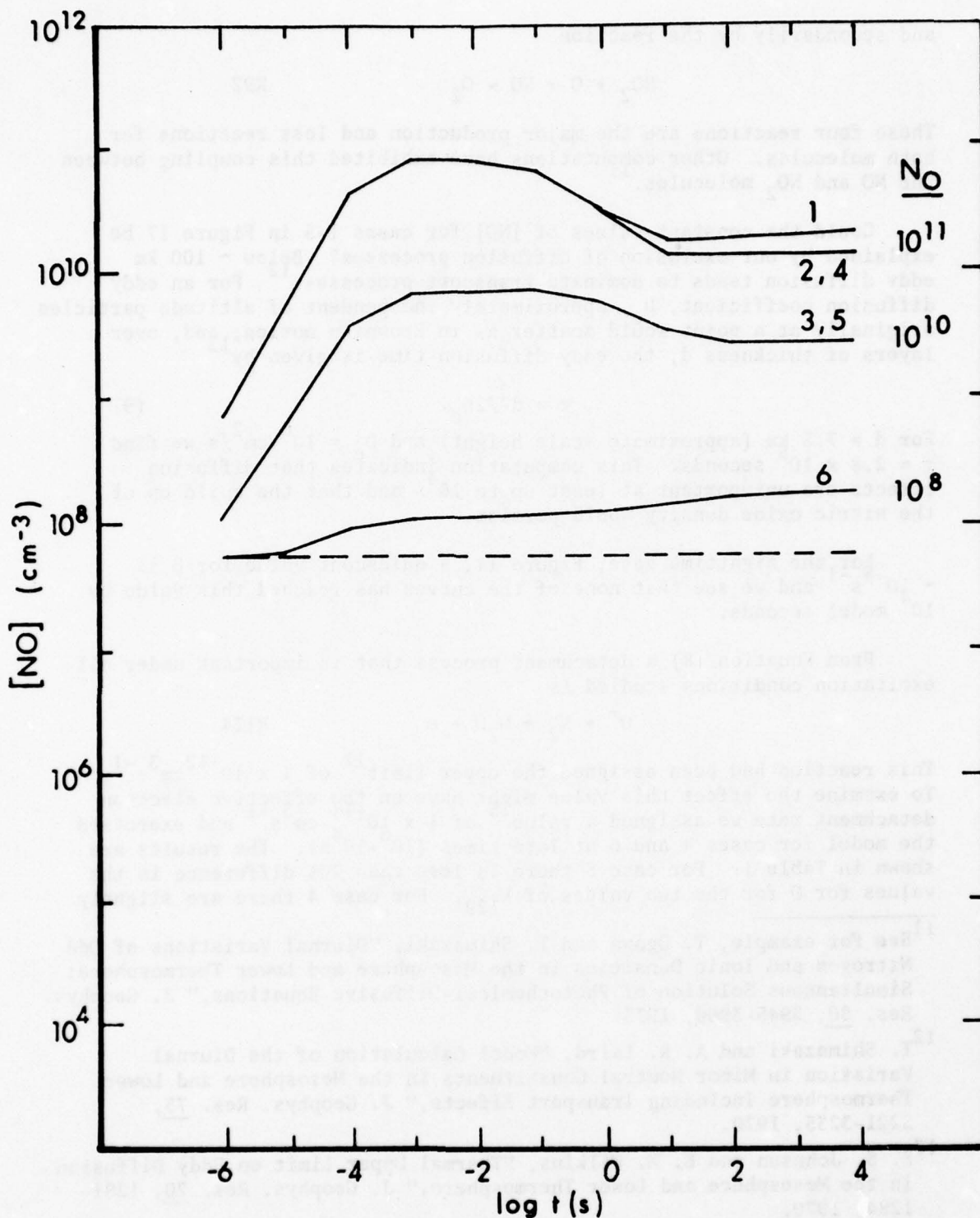


Figure 17. History of the nitric oxide density at 60 km. The dashed line denotes the quiescent value. The numbers refer to excitation conditions whose key may be found listed in the figures. The column to the far right of the curves lists the values of prompt ionization parameter,  $N_0$ , clearly showing the correlation between the value of this parameter and the late time value computed for nitric oxide.

and secondarily by the reaction



R92

These four reactions are the major production and loss reactions for both molecules. Other computations have exhibited this coupling between the NO and NO<sub>2</sub> molecules.<sup>11</sup>

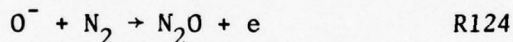
Could the constant values of [NO] for cases 1-5 in Figure 17 be explained by our exclusion of diffusion processes? Below ~ 100 km eddy diffusion tends to dominate transport processes.<sup>12</sup> For an eddy diffusion coefficient, D<sub>e</sub>, approximately independent of altitude particles originally at a point would scatter as in Brownian motion;<sup>13</sup> and, over layers of thickness d, the eddy diffusion time is given by<sup>13</sup>

$$\tau = d^2/2D_e. \quad (9)$$

For d = 7.5 km (approximate scale height) and D<sub>e</sub> = 10<sup>6</sup> cm<sup>2</sup>/s we find  $\tau = 2.8 \times 10^5$  seconds. This computation indicates that diffusion effects are unimportant at least up to 10<sup>4</sup> s and that the build up of the nitric oxide density would persist.

For the nighttime case, Figure 14, a quiescent value for D is ~ 10<sup>-8</sup> s<sup>-1</sup> and we see that none of the curves has reached this value by 10<sup>6</sup> model seconds.

From Equation (8) a detachment process that is important under all excitation conditions studied is



This reaction had been assigned the upper limit<sup>14</sup> of  $1 \times 10^{-12} \text{ cm}^3 \text{ s}^{-1}$ . To examine the effect this value might have on the effective electron detachment rate we assigned a value<sup>15</sup> of  $1 \times 10^{-14} \text{ cm}^3 \text{ s}^{-1}$  and exercised the model for cases 4 and 6 at late times (10<sup>0</sup>-10<sup>4</sup> s). The results are shown in Table 1. For case 6 there is less than 20% difference in the values for D for the two values of k<sub>129</sub>. For case 4 there are slightly

<sup>11</sup>See for example, T. Ogawa and T. Shimazaki, "Diurnal Variations of Odd Nitrogen and Ionic Densities in the Mesosphere and Lower Thermosphere: Simultaneous Solution of Photochemical-Diffusive Equations," J. Geophys. Res. 80, 3945-3960, 1975.

<sup>12</sup>T. Shimazaki and A. R. Laird, "Model Calculation of the Diurnal Variation in Minor Neutral Constituents in the Mesosphere and Lower Thermosphere Including Transport Effects," J. Geophys. Res. 75, 3221-3235, 1970.

<sup>13</sup>F. S. Johnson and E. M. Wilkins, "Thermal Upper Limit on Eddy Diffusion in the Mesosphere and Lower Thermosphere," J. Geophys. Res. 70, 1281-1284, 1970.

<sup>14</sup>W. Lindinger, D. C. Albritton, F. C. Fehsenfeld and E. E. Ferguson, "Reactions of O<sup>-</sup> with N<sub>2</sub>, N<sub>2</sub>O, SO<sub>2</sub>, NH<sub>3</sub>, CH<sub>4</sub> and C<sub>2</sub>H<sub>4</sub> and C<sub>2</sub>H<sub>2</sub><sup>-</sup> with O from 300°K to Relative Kinetic Energies of ~ 2 eV," J. Chem. Phys. 63, 3238-3242, 1975.

<sup>15</sup>F. C. Fehsenfeld, private communication, 1977.

TABLE 1. COMPUTED VALUES OF  $D$  ( $s^{-1}$ ) AS A FUNCTION OF TIME AND VALUE OF  $k_{129}$  FOR CASE 6<sup>†</sup> AND CASE 4<sup>\*</sup>

CASE	$k_{129}$ (cc/s)	time (s)	$10^0$	$10^1$	$10^2$	$10^3$	$10^4$
6	$10^{-12}$		8.89(-1) <sup>**</sup>	1.06(0)	9.17(-1)	8.60(-1)	8.97(-1)
6	$10^{-14}$		7.58(-1)	8.95(-1)	7.77(-1)	7.50(-1)	7.84(-1)
4	$10^{-12}$		8.14(+1)	3.38(+1)	4.98(0)	9.77(-1)	3.23(-2)
4	$10^{-14}$		5.58(+1)	2.27(+1)	2.88(0)	7.61(-1)	2.92(-2)

$$^{\dagger}Q_0 = 10^6 \text{ ion pairs cm}^{-3}\text{s}^{-1}, N_0 = 10^8 \text{ cm}^{-3}$$

$$^*Q_0 = 10^6 \text{ ion pairs cm}^{-3}\text{s}^{-1}, N_0 = 10^{11} \text{ cm}^{-3}$$

<sup>\*\*</sup>Read as  $8.89 \times 10^{-1}$ .

differing rates of decline for the two values of  $k_{129}$  resulting in a maximum of 53% difference at  $10^2$  seconds. As we have found previously,<sup>10</sup> with the smaller value for  $k_{129}$ , reaction 129 was no longer dominant, but was still significant ( $> 10\%$ ) and could not in general be ignored.

The effective recombination coefficient is defined by

$$\psi = (1 + \lambda)(\alpha_d + \lambda\alpha_i), \quad (9)$$

where  $\lambda$  is the ratio of the total negative ion density to the electron density and  $\alpha_i$  is the effective positive ion-negative ion recombination coefficient.<sup>11</sup> In the steady state, a criterion many times employed in hybrid models,<sup>16</sup>  $\psi$  (solid lines in Figures 18 and 19), should equal the source term divided by the electron density squared,  $Q/[e]^2$  (dashed lines in Figures 18 and 19). This equality is approximately reached (i.e., within 20%) in both Figures 18 and 19 by  $10^{-1}$ s for curve 1, by  $10^0$ s for curves 2 and 3 and by  $10^2$ s for curves 4, 5 and 6 (by  $10^3$ s for curve 6 at night). These curves tend to be grouped according to the value of  $Q_0$ . We have not been able to find a simple explanation as to why this is so.

The governing equation for the approach to the steady state is

$$d[e]/dt = Q(t) - \psi\{\alpha_d(Q), \lambda(Q), \alpha_i(t)\}[e]^2, \quad (10)$$

where  $Q$  and  $\psi$  are given by equations (1) and (9), respectively. The explicit dependencies are written out to emphasize the fact that  $\psi$  is an implicit function of time through  $Q$ . From equation (10), one might expect the tendency to group the time at which a steady state condition is reached with  $Q_0$ , as observed in Figures 18 and 19. But, the non-linearity and implicit functional dependencies upon time in equation (10) have prevented any simple qualitative understanding of the observed grouping with  $Q_0$ . Several attempts to solve simpler formulations of equation (10) indicate that these simpler solutions would not reproduce the computed results of Figures 18 and 19. In other words to attain the results observed in Figures 18 and 19, we have found that equation (10) should be solved in its entirety, as is accomplished by the BENCHMARK-76 program.

#### SUMMARY

The BENCHMARK-76 code has been employed to obtain species densities as a function of time and excitation conditions for an altitude of 60 km. The excitation conditions employed were as follows. The prompt ionization,  $N_0$ , was assigned the values  $10^{11}$ ,  $10^{10}$  or  $10^8$   $\text{cm}^{-3}$ , and the delayed ionization is given by  $Q(t) = Q_0(1 + t)^{-1.2}$  where  $t$  is the time

<sup>16</sup> See for example, A. P. Mitra, "D-Region in Disturbed Condition, Including Flares and Energetic Particles," J. Atmos. and Terr. Phys. 37, 895-913, 1975.

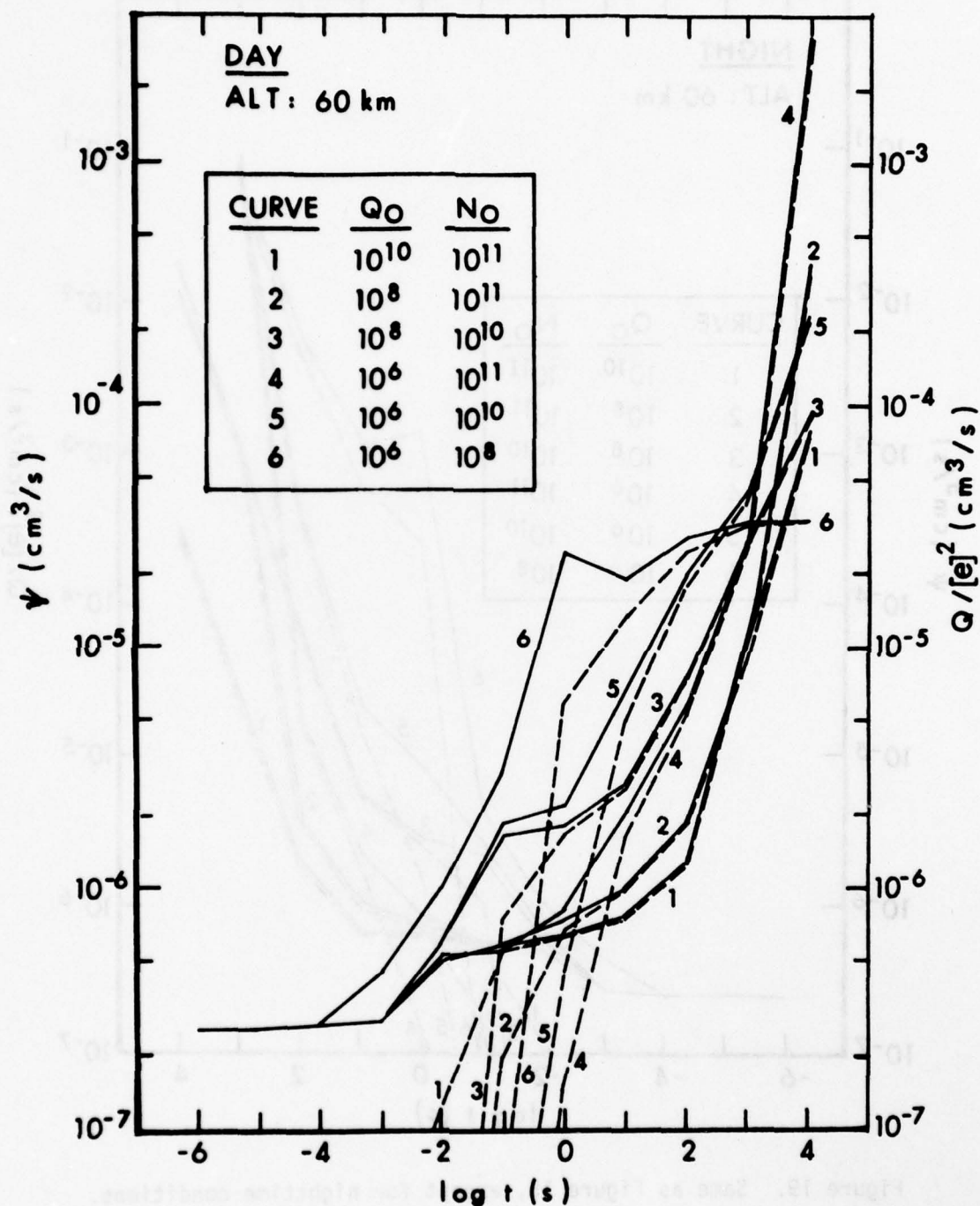


Figure 18. Composite plot of the logarithm of the total recombination coefficient,  $\psi$  (solid line), and of  $Q/[e]^2$  (dashed line), as a function of the logarithm of time. Conditions are daytime at 60 km for the six different excitation parameters shown.

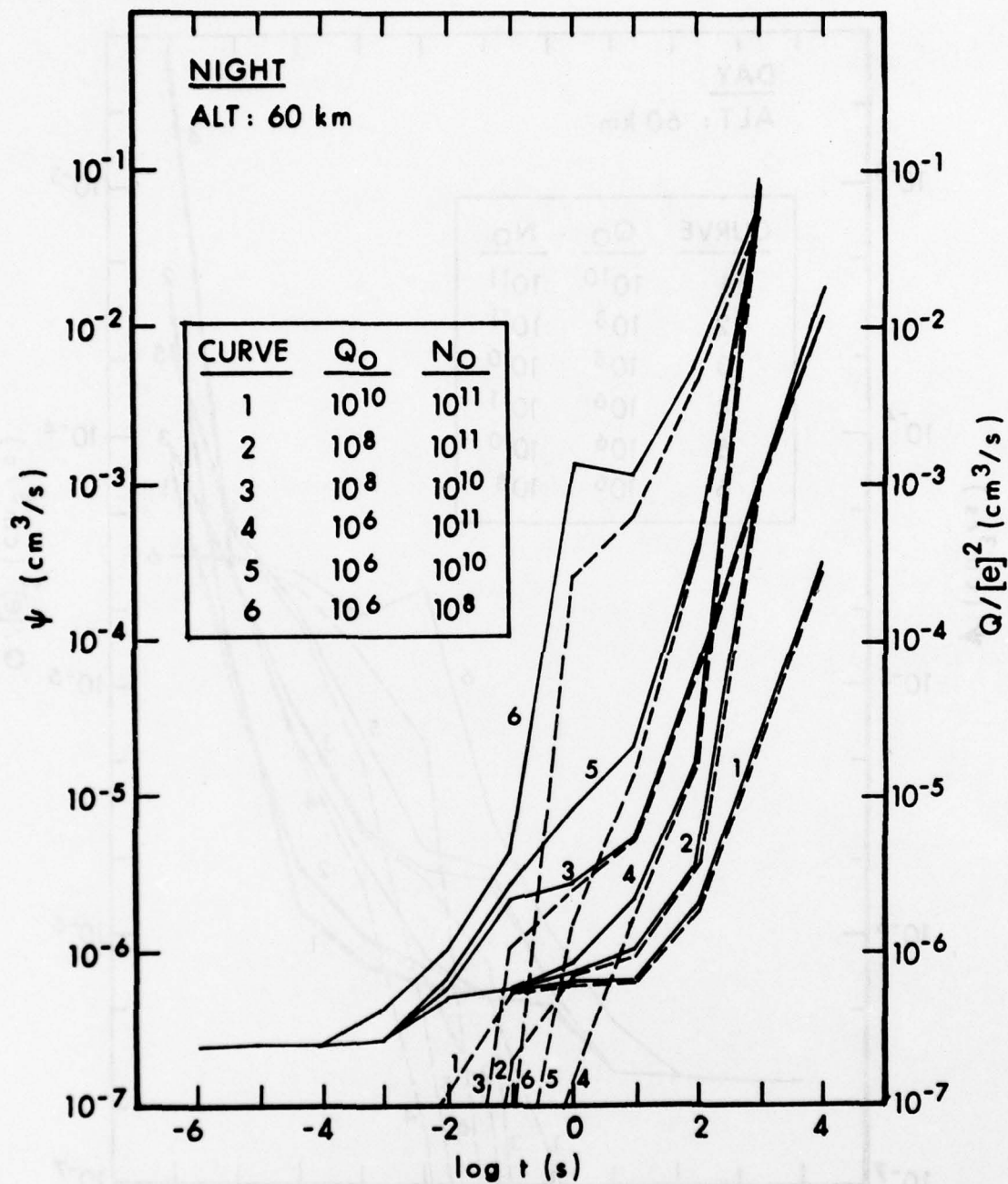


Figure 19. Same as Figure 15, except for nighttime conditions.

in seconds and  $Q_0$  assigned the values of  $10^6$ ,  $10^8$  or  $10^{10}$  ion-pairs  $\text{cm}^{-3} \text{s}^{-1}$ , subject to the constraint  $|Q_0| < |N_0|$ . Computations were made for three hour intervals around noon (DAY) and midnight (NIGHT). Analysis of these calculations is summarized as follows.

First, for a given delayed ionization parameter,  $Q_0$ , it is found that the greater the initial ionization parameter,  $N_0$ , the sooner the electron density relaxes to its quiescent value. This inversion of one's intuitive feeling is traced to severe neutral chemistry changes that affect the negative ion chemistry.

Second, the comparison between the BENCHMARK-76 (BRL) and the DCHEM (MRC) calculations of the electron densities at  $360 \text{ km}$  for both day and night conditions and for  $Q_0 = 10^6$  ion-pairs  $\text{cm}^{-3} \text{s}^{-1}$  and  $N_0 = 10^8$  or  $10^{10} \text{ cm}^{-3}$  are good to excellent.

Third, the calculated relaxation of the effective electron-ion recombination coefficient to quiescent values is dominated by  $Q_0$ , i.e., the larger  $Q_0$  the longer the relaxation time. The return to quiescent values for the higher excitation conditions is computed to take longer than  $10^4$  seconds.

Fourth, variations in the effective electron attachment frequency,  $A$ , amounting to almost a factor of two at night, are traced in detail and found to result from ozone enhancement at late times.

Fifth, only the daytime effective electron recombination coefficient for the mildest excitation studied is found to relax to a typical quiescent value. In the daytime, all other, stronger excitation cases indicate a relaxation to values much below that expected for quiescent conditions. This phenomenon is traced to the greater build up in the nitric oxide density with the larger value of  $N_0$ . In the nighttime cases, no curves approach their quiescent values even after  $10^3$  or  $10^4 \text{ s}$ . We have found that the reaction  $\text{O}^- + \text{N}_2 \rightarrow \text{N}_2\text{O} + \text{e}$  is non-negligible, even when its rate coefficient is reduced one hundredfold to  $10^{-14} \text{ cm}^3/\text{s}$ .

Finally, the time to attain a steady state condition as measured by the criterion  $\psi = Q/[e]^2$ , is found to be a function of  $Q_0$ . The smaller this parameter, the longer it takes to reach the steady state. Attempts to understand this behavior by simplifying the governing non-linear differential equation for the electron density were not successful, but, led us to the conclusion that, in order to obtain these results, this equation ought to be solved in its entirety, as is accomplished by the BENCHMARK-76 program.

#### ACKNOWLEDGEMENT

To M. G. Heaps and G. E. Keller goes our thanks for reading an earlier version of this manuscript.

## REFERENCES

1. E. L. Lortie, M. D. Kregel and F. E. Niles, "AIRCHEM: A Computational Technique for Modeling the Chemistry of the Atmosphere," BRL Report No. 1913, August 1976. (AD# A030157)
2. F. Gilmore as quoted by B. F. Myers and M. R. Schoonover, "Electron Energy Degradation in the Atmosphere: Consequent Species and Energy Densities, Electron Flux, and Radiation Spectra," DNA 3513T, 3 Jan 75, Table 6.
3. J. M. Heimerl and F. E. Niles, "BENCHMARK-76: Model Computations for Disturbed Atmospheric Conditions I. Input Parameters," BRL Report No. 2022, October 1977. (AD #A050355)
4. F. E. Niles and J. M. Heimerl, "Selected Neutral Species Profiles 0-100 km," BRL Memo Report 2767, July 1977. (AD# A042620)
5. See for example E. E. Ferguson, D. B. Dunkin and F. C. Fehsenfeld, "Reactions of  $\text{NO}_2^-$  and  $\text{NO}_3^-$  with HCl and HBr," J. Chem. Phys. 57, 1459-1463, 1972.
6. R. J. Celotta, R. A. Bennett, J. L. Hall, M. W. Siegel and J. Levine, "Molecular Photodetachment Spectrometry. II. The Electron Affinity of  $\text{O}_2$  and the Structure of  $\text{O}_2^-$ ," Phys. Rev. A6, 631-642, 1972.
7. S. P. Hong, S. B. Woo and E. M. Helmy, "Photodetachment of Thermally Relaxed  $\text{CO}_3^-$ ," Phys. Rev. A15, 1563-1569, 1977.
8. W. S. Knapp, "A Simplified D-Region Chemistry Model for Nuclear Environments," DNA 2850T, April 72; also M. Scheibe, private communication, 1976.
9. For example, the BENCHMARK-76 reaction set includes neutral odd-hydrogen reactions; Scheibe's set does not.
10. J. M. Heimerl and F. E. Niles, "BENCHMARK-76: Model Computations for Disturbed Atmospheric Conditions II. Results for the Stratosphere and Mesosphere," BRL Technical Report ARBRL-TR-02050, March 1978.
11. See for example, T. Ogawa and T. Shimazaki, "Diurnal Variations of Odd Nitrogen and Ionic Densities in the Mesosphere and Lower Thermosphere: Simultaneous Solution of Photochemical-Diffusive Equations," J. Geophys. Res. 80, 3945-3960, 1975.
12. T. Shimazaki and A. R. Laird, "Model Calculation of the Diurnal Variation in Minor Neutral Constituents in the Mesosphere and Lower Thermosphere Including Transport Effects," J. Geophys. Res. 75, 3221-3235, 1970.

#### REFERENCES (CONTD)

13. F. S. Johnson and E. M. Wilkins, "Thermal Upper Limit on Eddy Diffusion in the Mesosphere and Lower Thermosphere," J. Geophys. Res. 70, 1281-1284, 1970.
14. W. Lindinger, D. C. Albritton, F. C. Fehsenfeld and E. E. Ferguson, "Reactions of  $O^-$  with  $N_2$ ,  $N_2O$ ,  $SO_2$ ,  $NH_3$ ,  $CH_4$  and  $C_2H_4$  and  $C_2H_2^-$  with O from 300°K to Relative Kinetic Energies of  $\sim 2$  eV," J. Chem. Phys. 63, 3238-3242, 1975.
15. F. C. Fehsenfeld, private communication, 1977.
16. See for example, A. P. Mitra, "D-Region in Disturbed Condition, Including Flares and Energetic Particles," J. Atmos. and Terr. Phys. 37, 895-913, 1975.

## APPENDIX

The table in this Appendix displays the nominal 496 reactions that link the 64 species within the BENCHMARK-76 code. Reactions proceed from left to right only. Each rate coefficient,  $k$ , is constructed from the reaction parameters A, B and C, i.e.

$$k = A(T/300)^B \exp (- C/T) ,$$

where T is the temperature in degrees Kelvin. Except for the first 60 reactions, involving a photon as a reactant, the reference for the value of the rate coefficient is given to the right of the parameter C column. Further details can be obtained from Reference 3.

TABLE A. BENCHMARK-76 REACTION SET

REF. NO.	REACTION	WAVELENGTH REGION	REFERENCE
1	NO2 + HV = NO2 + E		
2	O + HV = O + E		
3	O + HV = O1D + E		
4	O2 + HV = O2 + E		
5	O3 + HV = O3 + E		
6	CO3 + HV = CO2 + O + E		
7	CO4 + HV = CO3 + H2O		
8	CO4 + HV = CO2 + CO2		
9	CO4 + HV = CO4 + H2O		
10	CO4 + HV = NO2 + H2O		
11	NO3 + HV = O + NO2 + E		
12	NO3 + HV = NO + O2 + E		
13	NO3 + HV = NO3 + H2O		
14	NO3 + HV = NO3 + HNO3		
15	NO3 + HV = O2 + H2O		
16	NO3 + HV = O2 + O2		
17	NO4 + HV = NO + CO2		
18	NO4 + HV = NO + H2O		
19	NO4 + HV = NO + H2		
20	NO5 + HV = NO + H2		
21	NO5 + HV = NO4 + CO2		
22	NO6 + HV = H3O + HNO2		
23	NO6 + HV = NO4 + H2O		
24	NO6 + HV = NO4 + H2		
25	NO6 + HV = NO4 + CO2		
26	NO8 + HV = NO6 + H2O		
27	NO9 + HV = NO6 + H2		
28	NO9 + HV = NO2 + H2O		
29	NO9 + HV = NO2 + H2		
30	NO9 + HV = NO2 + H2		
31	NO9 + HV = NO2 + H2		
32	NO9 + HV = NO2 + H2		
33	NO9 + HV = NO2 + H2		
34	NO9 + HV = NO2 + H2		
35	NO9 + HV = NO2 + H2		
36	NO9 + HV = NO2 + H2		
37	NO9 + HV = NO2 + H2		
38	NO9 + HV = NO2 + H2		
39	NO9 + HV = NO2 + H2		
40	NO9 + HV = NO2 + H2		
41	NO9 + HV = NO2 + H2		
42	NO9 + HV = NO2 + H2		
43	NO9 + HV = NO2 + H2		
44	NO9 + HV = NO2 + H2		
45	NO9 + HV = NO2 + H2		
46	NO9 + HV = NO2 + H2		
47	NO9 + HV = NO2 + H2		
48	NO9 + HV = NO2 + H2		
49	NO9 + HV = NO2 + H2		
50	NO9 + HV = NO2 + H2		
51	NO9 + HV = NO2 + H2		
52	NO9 + HV = NO2 + H2		
53	NO9 + HV = NO2 + H2		
54	NO9 + HV = NO2 + H2		
55	NO9 + HV = NO2 + H2		
56	NO9 + HV = NO2 + H2		
57	NO9 + HV = NO2 + H2		
58	NO9 + HV = NO2 + H2		
59	NO9 + HV = NO2 + H2		
60	NO9 + HV = NO2 + H2		

REAC. NO.	REACTION	A	B	C	REFERENCE	REF. NO.
61	H + H2O2 = H + H2O	5.3E-10	.0	4500	BAULCH ETAL HI TEMP REAC RATE DATA, LEEDS	69
62	H + H2O2 = H2 + H2O	2.8E-12	.0	1900	HAMPSON + GBSIR-73-207 AUG 73	61
63	H + H2O = H2 + O	4.2E-12	1.0	3500	HAMPSON + GARVIN-ED NBS-TN-866	62
64	H + H2O2 = H2 + O2	4.2E-11	.0	350	HAMPSON + GARVIN-ED NBS-TN-866	63
65	H + H2O2 = H2 + H2O	4.2E-10	.0	950	HAMPSON + GARVIN-ED NBS-TN-866	64
66	H + H2O2 = H2O + O	8.5E-11	.0	500	HAMPSON + GARVIN-ED NBS-TN-866	65
67	H + H2O2 = H2O + H2O	5.8E-10	.0	740	HAMPSON + GARVIN-ED NBS-TN-866	66
68	H + H2O2 = H2O + H2O	1.3E-10	.0	740	HAMPSON + GARVIN-ED NBS-TN-866	67
69	H + H2O2 = H2O + H2O	3.7E-10	.0	8450	HAMPSON + GARVIN-ED NBS-TN-866	68
70	H + O2 = O + H2O	2.6E-11	.0	0	HAMPSON + GARVIN-ED NBS-TN-866	69
71	H + H2 = H + H2O	3.6E-11	.0	2590	HAMPSON + GARVIN-ED NBS-TN-866	70
72	H + H2O2 = H2O + H2O	1.7E-11	.0	910	HAMPSON + GARVIN-ED NBS-TN-866	71
73	H + HNO2 = H2O + H2O	2.1E-12	.0	0	HAMPSON + GARVIN-ED NBS-TN-866	72
74	H + HNO3 = H2O + H2O + O	1.3E-13	.0	0	HAMPSON + GARVIN-ED NBS-TN-866	73
75	H + H2O = H + H2O	1.0E-11	.0	550	HAMPSON + GARVIN-ED NBS-TN-866	74
76	H + H2O2 = H2O + O2	6.0E-11	.0	0	HAMPSON + GARVIN-ED NBS-TN-866	75
77	H + O3 = O2 + H2O	1.6E-12	.0	1000	HAMPSON + GARVIN-ED NBS-TN-866	76
78	H2O2 + H2O2 = H2O2 + O2	3.0E-11	.0	500	HAMPSON + GARVIN-ED NBS-TN-866	77
79	H2O2 + O3 = H2O + O2 + O2	1.0E-13	.0	1250	HAMPSON + GARVIN-ED NBS-TN-866	78
80	H + H2O = H + H2O	5.3E-11	.0	0	HAMPSON + GARVIN-ED NBS-TN-866	79
81	N + H2O = N2 + O	1.4E-11	.0	0	HAMPSON + GARVIN-ED NBS-TN-866	80
82	N + H2O = N2O + N2	1.4E-11	.0	0	HAMPSON + GARVIN-ED NBS-TN-866	81
83	N + H2O2 = H2O + O2	1.4E-12	.0	0	HAMPSON + GARVIN-ED NBS-TN-866	82
84	N + O2 = NO + O	3.3E-12	1.0	3150	HAMPSON + GARVIN-ED NBS-TN-866	83
85	N + O3 = NO + O2	5.7E-13	.0	0	HAMPSON + GARVIN-ED NBS-TN-866	84
86	N2O + O2 = NO + O	7.5E-12	.5	0	SLANGER, WOOD + BLACK JER 76, 8430 71	85
87	NO + H2O2 = H2O + H2O	2.0E-13	.0	0	HAMPSON + GARVIN-ED NBS-TN-866	86
88	NO + O3 = NO2 + O2	9.0E-13	.0	1200	HAMPSON + GARVIN-ED NBS-TN-866	87
89	O + H2O2 = H2O + H2O	2.8E-12	.0	2125	HAMPSON + GARVIN-ED NBS-TN-866	88
90	O + H2O = O2 + H2O	4.2E-11	.0	0	HAMPSON + GARVIN-ED NBS-TN-866	89
91	O + H2O2 = H2O + O2	8.0E-11	.0	500	HAMPSON + GARVIN-ED NBS-TN-866	90
92	O + H2O2 = H2O + O2	9.1E-12	.0	0	HAMPSON + GARVIN-ED NBS-TN-866	91
93	O + O3 = O2 + O2	1.0E-11	.0	2300	HAMPSON + GARVIN-ED NBS-TN-866	92
94	O + O3 = O2 + O2	1.0E-11	.0	2300	HAMPSON + GARVIN-ED NBS-TN-866	93
95	O1D + H2 = H2O + H	2.9E-10	.0	0	HAMPSON + GARVIN-ED NBS-TN-866	94
96	O1D + H2O = H2O + H2O	3.5E-11	.0	0	HAMPSON + GARVIN-ED NBS-TN-866	95
97	O1D + M = O + M	5.5E-11	.0	0	HAMPSON + GARVIN-ED NBS-TN-866	96
98	O1D + H2O = H2O + H2O	1.1E-10	.0	0	GARVIN-ED NBSIR 73-206 MAY 73	97
99	O1D + O2 = O + O2	7.4E-11	.0	0	HAMPSON + GARVIN-ED NBS-TN-866	98
100	O1D + O3 = O2 + O2	2.5E-10	.0	0	HAMPSON + GARVIN-ED NBS-TN-866	99
101	O21D + O2 = O2 + O2	2.2E-10	.8	0	HAMPSON + GARVIN-ED NBS-TN-866	100
102	O21D + O21U = O21S + O2	2.0E-18	.0	0	AKNOLD + OGRYZLO, CAN J PHYS 45, 2053 67	101
103	O21S + M = O2 + M	2.0E-15	.0	0	HAMPSON + GARVIN-ED NBS-TN-866	102
104	O21S + O3 = O + O2 + O2	2.5E-11	.0	0	GILPIN, SCHIFF + WELGE, J CHEM PHYS 55, 1087 71	103
105	H + H + M = H2 + M	8.3E-33	.0	0	HAMPSON + GARVIN-ED NBS-TN-866	104
106	H + H + M = H2O + M	6.8E-31	-2.0	0	HAMPSON + GARVIN-ED NBS-TN-866	105
107	H + O + M = H2O + M	2.0E-32	.0	0	HAMPSON + GARVIN-ED NBS-TN-866	106
108	H + O2 + M = H2O2 + M	2.1E-32	.0	-290	HAMPSON + GARVIN-ED NBS-TN-866	107
109	H + O + H2O = H2O2 + M	2.5E-33	.0	-2550	HAMPSON + GARVIN-ED NBS-TN-866	108
110	HO + H2O2 + M = HNO3 + M	2.2E-30	-2.5	0	HAMPSON + GARVIN-ED NBS-TN-866	109
111	HO + O + M = H2O + M	1.0E-31	.0	0	ESTIMATED	110
112	N + N + M = N2 + M	8.3E-34	.0	-500	HAMPSON + GARVIN-ED NBS-TN-866	111
113	N + O + M = NO + M	1.0E-32	-5	-526	HAMPSON + GARVIN-ED NBS-TN-866	112
114	NO + O2 + M = NO2 + M	3.3E-39	.0	-940	HAMPSON + GARVIN-ED NBS-TN-866	113
115	O + O + M = O2 + M	4.0E-33	.0	170	HAMPSON + GARVIN-ED NBS-TN-866	114
116	O + O2 + M = O3 + M	1.3E-32	-1.0	-510	HAMPSON + GARVIN-ED NBS-TN-866	115
117	O + O2 + M = O3 + M	1.1E-34	.0	0	HAMPSON + GARVIN-ED NBS-TN-866	116
118	O1D + N2 + M = N2O + M	2.8E-36	.0	0	HAMPSON + GARVIN-ED NBS-TN-866	117
119	O1D = O + HV	6.8E-03	.0	0	DNA HANDBOOK 1948H REV3 TABLE 24 REACTION XXX-1	118
120	O21D = O2 + HV	2.6E-04	.0	0	DNA HANDBOOK 1948H REV3 TABLE 24 REACTION XXX-5	119

REAC. NO.	REACTION	A	B	C	REFERENCE	REF. NO.
121	0215 = 02 + HV	8.3E-02	.0	0	DNA HANDBOOK 1948H REV3 TABLE 24 REACTION XXX-6	121
122	02 + E = N02-	4.0E-11	.0	0	DNA HANDBOOK REV3 TABLE 24 REACTION IX-7 SAT 38	122
123	HN03 + E = N02- + H0	5.0E-08	.0	0	FERGUSON ET AL DNA 3722F AUG 75	123
124	03 + E = 0- + 02	9.0E-12	1.5	0	DNA HANDBOOK REV3 TABLE 24 REACTION IX-1 1 CHAN	124
125	02 + E + 02 = 02- + 02	1.4E-29	-1.0	600	DNA HANDBOOK REV3 TABLE 24 REACTION IX-2	125
126	02 + E + N2 = H20 + E	1.0E-31	.0	0	DNA HANDBOOK REV3 TABLE 24 REACTION IX-3	126
127	0- + H2 = H20 + E	6.0E-10	-2	0	MCFARLAND ETAL J CHEM PHYS 59.6629 73	127
128	0- + N = N0 + E	2.2E-10	.0	0	DNA HANDBOOK	128
129	0- + N2 = N20 + E	1.0E-12	.0	0	LINDINGER ETAL J CHEM PHYS 63.3238.75 UP LIM	129
130	0- + N0 = N02 + E	2.5E-10	-8	0	MCFARLAND ETAL J CHEM PHYS 59.6629 73	130
131	0- + 0 = 02 + E	2.0E-10	.0	0	DNA HANDBOOK REV3 TABLE 24 REACTION XII-1	131
132	02- + N = N02 + E	3.0E-10	.0	0	DNA HANDBOOK REV3 TABLE 24 REACTION XII-3	132
133	02- + N2 = 02 + E + N2	3.0E-10	.0	0	FENSENFELD, PRIVATE COMMUNICATION	133
134	02- + 0 = 03 + E	1.9E-12	1.5	4990	DNA HANDBOOK REV3 TABLE 24 REACTION X-4	134
135	02- + 02 = 02 + E + 02	1.5E-10	.0	0	F. C. FENSENFELD, PRIVATE COMMUNICATION 75.	135
136	02- + 0210 = 02 + E + 02	2.7E-10	.5	5590	DNA HANDBOOK REV3 TABLE 24 REACTION X-5	136
137	02- + 0210 = 02 + E + 02	2.0E-10	.0	0	DNA HANDBOOK REV3 TABLE 24 REACTION X-6	137
138	H30+ + E = H + H20	1.3E-06	-2	0	DNA HANDBOOK REV4 TABLE 16-1	138
139	H37 + E = H + H20 + H20	2.8E-06	-2	0	DNA HANDBOOK REV4 TABLE 16-1	139
140	H36 + E = H20 + H + H0	3.0E-06	-1.0	0	DNA HANDBOOK	140
141	H47 + E = H + H20 + N2	1.0E-06	-2	0	ESTIMATED	141
142	H55 + E = H + H20 + H20	5.1E-06	-2	0	DNA HANDBOOK REV4 TABLE 16-1	142
143	H73 + E = H + H20 + H20 + H20	6.1E-06	-2	0	DNA HANDBOOK REV4 TABLE 16-1	143
144	H91 + E = H + H20 + H20 + H20 + H20	7.4E-06	-2	0	DNA HANDBOOK REV4 TABLE 16-1	144
145	N0+ + E = 0 + N	1.0E-07	-1.0	0	DNA HBK REV4 TABLE 16-1 KLEY ETAL JCP 66.4157.7	145
146	N0+ + E = 0 + N2U	3.0E-07	-1.0	0	DNA HANDBOOK, EST.	146
147	N074 + E = N0 + C02	1.0E-06	-2	0	DNA HANDBOOK, EST.	147
148	N08 + E = N0 + H20	1.0E-06	-2	0	DNA HANDBOOK, EST.	148
149	N058 + E = N0 + N2	1.0E-06	-2	0	DNA HANDBOOK, EST.	149
150	N092 + E = N0 + H20 + C02	1.0E-06	-2	0	DNA HANDBOOK, EST.	150
151	N066 + E = N0 + H20 + H20	2.0E-06	-2	0	DNA HANDBOOK, EST.	151
152	N076 + E = N0 + H20 + N2	1.0E-06	-2	0	DNA HANDBOOK, EST.	152
153	N110 + E = N0 + H20 + H20 + C02	1.0E-06	-2	0	DNA HANDBOOK, EST.	153
154	N084 + E = N0 + H20 + H20 + H20	3.0E-06	-2	0	DNA HANDBOOK REV3 TABLE 24 REACTION IV-10	154
155	N094 + E = N0 + H20 + H20 + N2	1.0E-06	-2	0	DNA HANDBOOK, EST.	155
156	N024 + E = N0 + 0	3.0E-07	-5	0	DNA HANDBOOK REV3 TABLE 24 REACTION IV-6 EST	156
157	64+ + E = N02 + H20	1.0E-06	-5	0	DNA HANDBOOK, EST.	157
158	62+ + E = N02 + H2J + H20	2.0E-06	-5	0	DNA HANDBOOK, EST.	158
159	N24 + E = N + N2U	2.7E-07	.0	0	DNA HANDBOOK REV4 FIGURE 16-1 ESTIMATED PRODUCT	159
160	02+ + E = 0 + 01U	2.1E-07	-7	0	DNA HANDBOOK, TABLE 24-1.	160
161	0250 + E = 02 + H20	1.5E-06	-2	0	DNA HANDBOOK, EST.	161
162	04+ + E = 02 + 02	2.0E-06	-1.0	0	DNA HANDBOOK REV3 TABLE 24 REACTION IV-11	162
163	N+ + 02 = N + 02+	2.9E-10	.0	0	MCFARLAND ETAL J C P 59.6620 73 TC4600.8/R=5	163
164	N2+ + 02 = N2 + 02+	5.0E-11	-8	0	MCFARLAND ETAL J CHEM PHYS 59.6620 73 TC3560	164
165	N02+ + N0 = N02 + N0+	2.9E-10	.0	0	DNA HANDBOOK REV3 TABLE 24 REACTION XIII-27	165
166	64+ + N0 = N048 + H02	1.0E-10	.0	0	DNA HANDBOOK, EST.	166
167	82+ + N0 = N066 + N02	1.0E-10	.0	0	DNA HANDBOOK, EST.	167
168	0+ + 02 = 0 + 02+	2.0E-11	-4	0	MCFARLAND ETAL J CHEM PHYS 59.6620 73 TC1800	168
169	02+ + N0 = 02 + N0+	4.4E-10	.0	0	LINDINGER ETAL JGR 80.3725 75	169
170	02+ + N02 = 02 + N02+	6.6E-10	.0	0	DNA HANDBOOK REV3 TABLE 24 REACTION XIII-16	170
171	0250 + N02 = 02 + H20 + N02+	1.0E-10	.0	0	DNA HANDBOOK REV3 TABLE 24 REACTION XIV-26 EST	171
172	04+ + N0 = 02 + 02 + N0+	1.0E-10	.0	0	ESTIMATED	172
173	04+ + N02 = 02 + 02 + N02+	5.0E-10	.0	0	DNA HANDBOOK REV3 TABLE 24 REACTION XIV-23 EST	173
174	04+ + N03 = 64+ + H20	5.0E-10	.0	0	ESTIMATED	174
175	H30+ + H03 = 64+ + H20	1.6E-09	.0	0	FENSENFELD ETAL J CHEM PHYS 63.2835 75	175
176	H36 + H20 = H37 + H0	1.4E-09	.0	0	DNA HANDBOOK REV3 TABLE 24 REACTION XIV-33	176
177	H47 + H20 = H37 + N2	1.0E-09	.0	0	ESTIMATED	177
178	N+ + 02 = N0+ + 0	2.8E-10	.0	0	MCFARLAND ETAL J C P 59.6620.73 TC4600.8/R=5	178
179	N074 + H20 = N048 + C02	1.0E-09	.0	0	ESTIMATED	179
180	N048 + H02 = H30+ + N0 + 02	5.0E-10	.0	0	ESTIMATED, ANALOGY WITH N048 + H202	180

REAC. NO.	REACTION	A	B	C	REFERENCE	REF. NO.
181	N048 + H0 = H30+ + N02	6.0E-11	.0	0	FEHSENFELD + FERGUSON RAD SCI 7.113 72 UP-LIM	181
182	N048 + H202 = H30+ + N02 + H0	3.0E-11	.0	0	ESTIMATED	182
183	N048 + H202 = N02+ + H20 + H20	3.0E-11	.0	0	ESTIMATED	183
184	N048 + H202 = 64+ + H20	3.0E-11	.0	0	ESTIMATED	184
185	N058 + C02 = N074 + N2	1.0E-09	.0	0	ESTIMATED	185
186	N058 + H20 = N048 + N2	1.0E-09	.0	0	ESTIMATED	186
187	N092 + H20 = N066 + C02	1.0E-09	.0	0	ESTIMATED	187
188	N076 + C02 = N092 + N2	1.0E-09	.0	0	ESTIMATED	188
189	N110 + H20 = N084 + C02	1.0E-09	.0	0	ESTIMATED	189
190	N084 + H20 = H+55 + HN02	7.0E-11	.0	0	DNA HANDBOOK REV3 TABLE 24 REACTION XIV-30	190
191	N094 + C02 = N110 + N2	1.0E-09	.0	0	ESTIMATED	191
192	64+ + N0 = N048 + N02	3.1E-11	.0	0	FEHSENFELD ETAL J CHEM PHYS 63.2835 75	192
193	82+ + H20 = H+37 + HN03	1.0E-10	.0	0	FEHSENFELD ETAL J CHEM PHYS 63.2835 75 LOW LIM	193
194	N2+ + 0 = N20 + N0+	1.0E-11	-2	0	MCFARLAND ETAL JGR 79.2925 74 B/R EST.	194
195	N2+ + 0 = N0+ + N	1.3E-10	-4	0	MCFARLAND ETAL JGR 79.2925 74 B/R EST.	195
196	0+ + N2 = N0+ + N	1.2E-12	-1.0	0	MCFARLAND ETAL J CHEM PHYS 59.6620 73	196
197	02+ + N = N0+ + 0	1.8E-10	.0	0	DNA HANDBOOK	197
198	02+ + N2 = N0+ + N0	1.0E-16	.0	0	DNA HANDBOOK REV3 TABLE 24 REACTION XIV-9 EST	198
199	0250 + H20 = H30+ + H0 + 02	2.0E-10	.0	0	DNA HANDBOOK REV3 TABLE 24 REACTION XIV-27A	199
200	0250 + H20 = H+36 + 02	1.0E-09	.0	0	DNA HANDBOOK REV3 TABLE 24 REACTION XIV-27B	200
201	0250 + 02 = 04+ + H20	2.0E-10	.0	2300	DNA HANDBOOK REV3 TABLE 24 REACTION XIV-25 EST	201
202	0260 + 02 = 04+ + N2	1.0E-09	.0	0	ESTIMATED	202
203	04+ + H20 = 0250 + 02	1.5E-09	.0	0	DNA HANDBOOK REV3 TABLE 24 REACTION XIV-24	203
204	04+ + 0 = 02+ + 03	3.0E-10	.0	0	DNA HANDBOOK REV3 TABLE 24 REACTION XIV-22	204
205	H30+ + H20 + M = H+37 + M	3.4E-27	.0	0	DNA HANDBOOK REV3 TABLE 24 REACTION XIX-13B	205
206	H30+ + N2 + M = H+47 + M	1.4E-30	-2.0	0	ESTIMATED	206
207	H37+ + H20 + M = H+55 + M	2.3E-27	-2.0	0	DNA HANDBOOK REV3 TABLE 24 REACTION XIX-14B	207
208	H55+ + H20 + M = H+73 + M	2.4E-27	-2.0	0	DNA HANDBOOK REV3 TABLE 24 REACTION XIX-15B	208
209	H73+ + H20 + M = H+91 + M	9.0E-28	-2.0	0	DNA HANDBOOK REV3 TABLE 24 REACTION XIX-16	209
210	N0+ + C02 + M = V074 + M	2.4E-29	-2.0	0	DNA HANDBOOK REV3 TABLE 24 REACTION XIX-10B	210
211	N0+ + H20 + M = N048 + M	1.5E-28	-2.0	0	DNA HANDBOOK REV3 TABLE 24 REACTION XIX-9	211
212	N0+ + N2 + M = N058 + M	2.0E-31	-4.4	0	JOHNSON ETAL J CHEM PHYS 63.3374 75	212
213	N048 + C02 + M = N092 + M	2.0E-29	-2.0	0	ESTIMATED	213
214	N048 + H20 + M = N066 + M	1.1E-27	-2.0	0	DNA HANDBOOK REV3 TABLE 24 REACTION XIX-11	214
215	N048 + N2 + M = N076 + M	2.0E-31	-4.4	0	ESTIMATED	215
216	N066 + C02 + M = N110 + M	2.0E-29	-2.0	0	ESTIMATED	216
217	N066 + H20 + M = N084 + M	1.6E-27	-2.0	0	DNA HANDBOOK REV3 TABLE 24 REACTION XIX-12	217
218	N066 + N2 + M = N094 + M	2.0E-31	-4.4	0	ESTIMATED	218
219	N02+ + H20 + M = 64+ + M	5.0E-28	-2.0	0	FEHSENFELD ETAL J CHEM PHYS 63.2835 75 TEMP EST	219
220	64+ + H20 + M = 82+ + M	2.0E-27	-2.0	0	FEHSENFELD ETAL J CHEM PHYS 63.2835 75 TEMP EST	220
221	0+ + N2 + M = N0+ + N + M	6.0E-29	-2.0	0	DNA HANDBOOK TABLE 18A-5 TAKE (1/82)---2,X3.8	221
222	02+ + H20 + M = 0250 + M	2.8E-28	-2.0	0	FEHSENFELD ETAL J CHEM PHYS 55.2115 71 MEN2	222
223	02+ + 02 + M = 04+ + M	3.9E-30	-3.2	0	PAYZANT ETAL J CHEM PHYS 59.5615 73	223
224	02+ + N2 + M = 0260 + M	9.0E-31	-2.0	0	DNA HANDBOOK TABLE 18A-5 TAKE (1/200)---2,X3.8	224
225	H36+ + M = H30+ + H0 + M	3.0E-03	-2.0	12000	ESTIMATED	225
226	H37+ + M = H30+ + H20 + M	1.6E 01	-2.0	18200	ESTIMATED	226
227	H47+ + M = H30+ + N2 + M	1.1E-08	-2.0	1900	ESTIMATED	227
228	H55+ + M = H+37 + H20 + M	1.6E-01	-2.0	11300	ESTIMATED	228
229	H73+ + M = H+55 + H20 + M	1.0E-01	-2.0	8600	ESTIMATED	229
230	H91+ + M = H+73 + H20 + M	1.3E 00	-2.0	7700	ESTIMATED	230
231	N074 + M = N0+ + N2 + C02 + M	7.8E-09	-4.4	5600	ESTIMATED	231
232	N058 + M = N048 + C02 + M	1.1E-08	-2.0	1900	J CHEM PHY 60. 4362. 74 + JCP 63. 3374. 75	232
233	N092 + M = N048 + H20 + M	5.9E-02	-2.0	5600	ESTIMATED	233
234	N066 + M = N048 + N2 + M	1.1E-08	-4.4	8700	ESTIMATED	234
235	N076 + M = N048 + C02 + M	4.0E-09	-2.0	1900	ESTIMATED	235
236	N110 + M = N066 + C02 + M	2.2E-02	-2.0	5600	ESTIMATED	236
237	N084 + M = N066 + H20 + M	1.0E-08	-4.4	7000	ESTIMATED	237
238	N094 + M = N066 + N2 + M	1.1E-08	-4.4	1900	ESTIMATED	238
239	0250 + 0210 = 02+ + 02 + H20	1.0E-10	.0	0	ESTIMATED	239
240	04+ + M = 02+ + 02 + M	1.2E-05	-3.2	5300	PAYZANT ETAL J CHEM PHYS 59. 5615. 73	240

REAC. NO.	REACTION	A	B	C	REFERENCE	REF. NO.
241	$\text{CO}_4^- + \text{O}_3 = \text{O}_3^- + \text{CO}_2 + \text{O}_2$	1.3E-10	0	0	0 FEHSENFELD + FERGUSON J CHEM PHYS 61.3181 74	241
242	$\text{O}^- + \text{NO}_2 = \text{O} + \text{NO}_2^-$	1.2E-09	0	0	0 DNA HANDBOOK REV3 TABLE 24 REACTION XV-2	242
243	$\text{O}^- + \text{O}_3 = \text{O} + \text{O}_3^-$	5.3E-10	0	0	0 DNA HANDBOOK REV3 TABLE 24 REACTION XV-3	243
244	$\text{O}_2^- + \text{NO}_2 = \text{O}_2 + \text{NO}_2^-$	1.2E-09	0	0	0 FEHSENFELD + FERGUSON J CHEM PHYS 61.3181 74	244
245	$\text{O}_2^- + \text{O} = \text{O}_2 + \text{O}^-$	1.5E-10	0	0	0 F. C. FEHSENFELD, PRIVATE COMMUNICATION 75.	245
246	$\text{O}_2^- + \text{O}_3 = \text{O}_2 + \text{O}_3^-$	4.0E-10	0	0	0 DNA HANDBOOK REV3 TABLE 24 REACTION XV-5	246
247	$\text{O}_2^- + \text{O}_3 = \text{O}_3^- + \text{O}_2$	2.3E-10	0	0	0 FEHSENFELD + FERGUSON J CHEM PHYS 61.3181 74	247
248	$\text{O}_4^- + \text{O}_3 = \text{O}_3^- + \text{O}_2 + \text{O}_2$	5.0E-10	0	0	0 ESTIMATED	248
249	$\text{CO}_3^- + \text{HNO}_3 = \text{NO}_3^- + \text{H}_2\text{O} + \text{CO}_2$	8.0E-10	0	0	0 FEHSENFELD ETAL J CHEM PHYS 63.2835 75	249
250	$\text{CO}_3^- + \text{O} = \text{NO}_2^- + \text{CO}_2$	9.0E-12	0	0	0 DNA HANDBOOK REV3 TABLE 24 REACTION XVI-23	250
251	$\text{CO}_3^- + \text{O}_2 = \text{NO}_3^- + \text{CO}_2$	2.0E-10	0	0	0 FEHSENFELD + FERGUSON J CHEM PHYS 61.3181 74	251
252	$\text{CO}_3^- + \text{O} = \text{O}_2 + \text{CO}_2$	8.0E-11	0	0	0 DNA HANDBOOK	252
253	$\text{CO}_3^- + \text{O} = \text{O}_2 + \text{CO}_2$	7.0E-12	0	0	0 FEHSENFELD + FERGUSON J CHEM PHYS 61.3181 74	253
254	$\text{CO}_3^- + \text{O} = \text{O}_2 + \text{CO}_2$	4.6E-11	0	0	0 DNA HANDBOOK REV3 TABLE 24 REACTION XVI-27	254
255	$\text{CO}_4^- + \text{O} = \text{CO}_3^- + \text{O}_2$	1.5E-10	0	0	0 DNA HANDBOOK REV3 TABLE 24 REACTION XVI-25	255
256	$\text{CO}_4^- + \text{O}_2 = \text{O}_4^- + \text{CO}_2$	4.3E-10	0	3000	0 DNA HANDBOOK REV3 TABLE 24 REACTION XVI-26 EST	256
257	$\text{O}_4^- + \text{O}_2 = \text{O}_4^- + \text{CO}_2$	5.0E-10	0	0	0 ESTIMATED	257
258	$\text{NO}_2^- + \text{HNO}_3 = \text{NO}_3^- + \text{HNO}_2$	1.6E-09	0	0	0 FEHSENFELD ETAL J CHEM PHYS 63.2835 75	258
259	$\text{NO}_2^- + \text{O}_2 = \text{NO}_3^- + \text{NO}$	2.0E-13	0	0	0 FEHSENFELD ETAL J CHEM PHYS 63.2835 75 UP LIM	259
260	$\text{NO}_2^- + \text{O}_3 = \text{NO}_3^- + \text{O}_2$	1.6E-11	0	0	0 DNA HANDBOOK REV3 TABLE 24 REACTION XVI-10	260
261	$\text{O}_4^- + \text{O}_3 = \text{O}_3^- + \text{O}_2$	5.0E-10	0	0	0 ESTIMATED	261
262	$\text{O}_4^- + \text{O}_3 = \text{O}_3^- + \text{O}_2$	1.5E-11	0	0	0 DNA HANDBOOK REV3 TABLE 24 REACTION XVI-15	262
263	$\text{O}_4^- + \text{HNO}_3 = \text{NO}_3^- + \text{H}_2\text{O}$	5.0E-10	0	0	0 FEHSENFELD ETAL J CHEM PHYS 63.2835 75 LOW LIM	263
264	$\text{O}_4^- + \text{HNO}_3 = \text{NO}_3^- + \text{H}_2\text{O}$	3.0E-09	0	0	0 FEHSENFELD ETAL J CHEM PHYS 63.2835 75	264
265	$\text{O}_2^- + \text{HNO}_3 = \text{NO}_3^- + \text{H}_2\text{O}$	2.6E-09	0	0	0 FEHSENFELD, PRIVATE COMMUNICATION	265
266	$\text{O}_2^- + \text{N} = \text{O} + \text{NO}$	1.0E-10	0	0	0 FEHSENFELD, PRIVATE COMMUNICATION	266
267	$\text{O}_2^- + \text{O}_2 = \text{CO}_4^- + \text{H}_2\text{O}$	5.6E-10	0	0	0 DNA HANDBOOK REV3 TABLE 24 REACTION XVI-21	267
268	$\text{O}_2^- + \text{O}_2 = \text{CO}_3^- + \text{H}_2\text{O}$	3.1E-10	0	0	0 DNA HANDBOOK REV3 TABLE 24 REACTION XVI-20	268
269	$\text{O}_3^- + \text{O}_2 = \text{CO}_3^- + \text{O}_2$	5.5E-10	0	0	0 FEHSENFELD + FERGUSON J CHEM PHYS 61.3181 74	269
270	$\text{O}_3^- + \text{O} = \text{NO}_2^- + \text{O}_2$	2.6E-12	0	0	0 F. C. FEHSENFELD, PRIVATE COMMUNICATION 75.	270
271	$\text{O}_3^- + \text{O}_2 = \text{NO}_3^- + \text{O}_2$	2.6E-10	0	0	0 DUNKIN ETAL CHEM PHYS LET 19.257 72	271
272	$\text{O}_3^- + \text{O} = \text{O}_2 + \text{O}_2$	3.2E-10	0	0	0 F. C. FEHSENFELD, PRIVATE COMMUNICATION 75.	272
273	$\text{O}_4^- + \text{O}_2 = \text{CO}_4^- + \text{O}_2$	4.3E-10	0	0	0 DNA HANDBOOK REV3 TABLE 24 REACTION XVI-19	273
274	$\text{O}_4^- + \text{H}_2\text{O} = \text{O}_2^- + \text{O}_2$	1.4E-09	0	0	0 DNA HANDBOOK REV3 TABLE 24 REACTION XVI-18	274
275	$\text{O}_4^- + \text{O} = \text{O}_3^- + \text{O}_2$	2.5E-10	0	0	0 DNA HANDBOOK REV3 TABLE 24 REACTION XVI-17	275
276	$\text{O}_4^- + \text{O} = \text{O}_3^- + \text{O}_2$	4.0E-10	0	0	0 DNA HANDBOOK REV3 TABLE 24 REACTION XVI-16	276
277	$\text{CO}_3^- + \text{H}_2\text{O} + \text{M} = \text{O}_3^- + \text{M}$	1.0E-28	-1.0	0	0 J CHEM PHYS 61.3181 74 M=O2 TEMP DEP ESTIMATED	277
278	$\text{CO}_4^- + \text{H}_2\text{O} + \text{M} = \text{O}_4^- + \text{M}$	5.0E-29	-1.0	0	0 ESTIMATED	278
279	$\text{NO}_2^- + \text{H}_2\text{O} + \text{M} = \text{O}_4^- + \text{M}$	1.3E-28	-1.0	0	0 DNA HANDBOOK REV3 TABLE 24 REACTION XXIII-11	279
280	$\text{NO}_3^- + \text{H}_2\text{O} + \text{M} = \text{O}_4^- + \text{M}$	7.5E-29	-1.0	0	0 PAYZANT, PRIVATE COMMUNICATION 72	280
281	$\text{O}^- + \text{CO}_2 + \text{M} = \text{O}_3^- + \text{M}$	3.1E-28	-1.0	0	0 J CHEM PHYS 61.3181 74 M=O2 TEMP DEP ESTIMATED	281
282	$\text{O}^- + \text{O}_2 + \text{M} = \text{O}_3^- + \text{M}$	1.1E-30	-1.0	0	0 PARKES, TRAN FAR SOC 67.711 71 M=O2 TEMP DEP EST	282
283	$\text{O}_2^- + \text{CO}_2 + \text{M} = \text{CO}_4^- + \text{M}$	2.0E-29	-1.0	0	0 DNA HANDBOOK REV3 TABLE 24 REACTION XXIII-9	283
284	$\text{O}_2^- + \text{H}_2\text{O} + \text{M} = \text{O}_2^- + \text{M}$	3.0E-28	-1.0	0	0 DNA HANDBOOK REV3 TABLE 24 REACTION XXIII-8	284
285	$\text{O}_4^- + \text{O}_2 + \text{M} = \text{O}_4^- + \text{M}$	3.5E-31	-1.0	0	0 DNA HANDBOOK REV3 TABLE 24 REACTION XXIII-6	285
286	$\text{H}_3\text{O}^+ + \text{O}_3^- = \text{H}_2\text{O} + \text{O}_2 + \text{M}$	2.0E-05	-1.0	6300	0 DNA HANDBOOK REV3 TABLE 24 REACTION XXIV-1	286
287	$\text{H}_3\text{O}^+ + \text{O}_3^- = \text{H}_2\text{O} + \text{O}_2 + \text{M}$	2.0E-07	-1.0	0	0 ESTIMATED	287
288	$\text{H}_3\text{O}^+ + \text{O}_3^- = \text{H}_2\text{O} + \text{O}_2 + \text{M}$	2.0E-07	-1.0	0	0 ESTIMATED	288
289	$\text{H}_3\text{O}^+ + \text{O}_4^- = \text{H}_2\text{O} + \text{O}_2 + \text{M}$	2.0E-07	-1.0	0	0 ESTIMATED	289
290	$\text{H}_3\text{O}^+ + \text{O}_4^- = \text{H}_2\text{O} + \text{O}_2 + \text{M}$	2.0E-07	-1.0	0	0 ESTIMATED	290
291	$\text{H}_3\text{O}^+ + \text{O}_2^- = \text{H}_2\text{O} + \text{O}_2 + \text{M}$	2.0E-07	-1.0	0	0 ESTIMATED	291
292	$\text{H}_3\text{O}^+ + \text{O}_4^- = \text{H}_2\text{O} + \text{O}_2 + \text{M}$	2.0E-07	-1.0	0	0 ESTIMATED	292
293	$\text{H}_3\text{O}^+ + \text{O}_3^- = \text{H}_2\text{O} + \text{O}_2 + \text{M}$	2.0E-07	-1.0	0	0 ESTIMATED	293
294	$\text{H}_3\text{O}^+ + \text{O}_2^- = \text{H}_2\text{O} + \text{O}_2 + \text{M}$	2.0E-07	-1.0	0	0 ESTIMATED	294
295	$\text{H}_3\text{O}^+ + \text{O}_2^- = \text{H}_2\text{O} + \text{O}_2 + \text{M}$	2.0E-07	-1.0	0	0 ESTIMATED	295
296	$\text{H}_3\text{O}^+ + \text{O}_2^- = \text{H}_2\text{O} + \text{O}_2 + \text{M}$	2.0E-07	-1.0	0	0 ESTIMATED	296
297	$\text{H}_3\text{O}^+ + \text{O}_2^- = \text{H}_2\text{O} + \text{O}_2 + \text{M}$	2.0E-07	-1.0	0	0 ESTIMATED	297
298	$\text{H}_3\text{O}^+ + \text{O}_2^- = \text{H}_2\text{O} + \text{O}_2 + \text{M}$	2.0E-07	-1.0	0	0 ESTIMATED	298
299	$\text{H}_3\text{O}^+ + \text{O}_2^- = \text{H}_2\text{O} + \text{O}_2 + \text{M}$	2.0E-07	-1.0	0	0 ESTIMATED	299
300	$\text{H}_3\text{O}^+ + \text{O}_3^- = \text{H}_2\text{O} + \text{O}_2 + \text{M}$	2.0E-07	-1.0	0	0 ESTIMATED	300



REAC. NO.	REACTION	A	B	C	REFERENCE	REF. NO.
361	N <sup>+</sup> + O <sup>+</sup> = H <sub>2</sub> O + H <sub>2</sub> O + H <sub>2</sub> O + H <sub>2</sub> O + H <sub>2</sub> O + H <sub>2</sub> O + O <sub>2</sub>	2.0E-07	-5	0	ESTIMATED	361
362	N <sup>+</sup> + CO <sub>2</sub> = NO + O + CO <sub>2</sub>	2.0E-07	-5	0	ESTIMATED	362
363	N <sup>+</sup> + 78- = CO <sub>2</sub> + O + H <sub>2</sub> O + NO	2.0E-07	-5	0	ESTIMATED	363
364	N <sup>+</sup> + CO <sub>4</sub> = CO <sub>2</sub> + O <sub>2</sub> + NO	2.0E-07	-5	0	ESTIMATED	364
365	N <sup>+</sup> + 94- = CO <sub>2</sub> + O <sub>2</sub> + H <sub>2</sub> O + NO	2.0E-07	-5	0	ESTIMATED	365
366	N <sup>+</sup> + NO <sub>2</sub> = NO <sub>2</sub> + NO	3.5E-07	-5	0	ESTIMATED	366
367	N <sup>+</sup> + 64- = NO <sub>2</sub> + H <sub>2</sub> O + NO	2.0E-07	-5	0	DNA HANDBOOK REV3 TABLE 24 REACTION V-8	367
368	N <sup>+</sup> + NO <sub>3</sub> = NO + NO <sub>2</sub> + O	2.0E-07	-5	0	ESTIMATED	368
369	N <sup>+</sup> + 62- = O <sub>2</sub> + NO + NO	4.0E-07	-5	0	DNA HANDBOOK REV3 TABLE 24 REACTION V-9	369
370	N <sup>+</sup> + 80- = NO <sub>2</sub> + H <sub>2</sub> O + NO + U	2.0E-07	-5	0	ESTIMATED	370
371	N <sup>+</sup> + 125- = HN03 + NO <sub>2</sub> + NO <sub>2</sub>	2.0E-07	-5	0	ESTIMATED	371
372	N <sup>+</sup> + O- = O + NO	4.5E-07	-5	0	DNA HANDBOOK REV3 TABLE 24 REACTION V-7	372
373	N <sup>+</sup> + O <sub>2</sub> = O <sub>2</sub> + NO	5.8E-07	-5	0	MOSELEY ETAL CASE STUDIES ATOMIC PHYS 5.1 75	373
374	N <sup>+</sup> + O <sub>2</sub> -W = O <sub>2</sub> + H <sub>2</sub> O + NO	2.0E-07	-5	0	ESTIMATED	374
375	N <sup>+</sup> + O <sub>3</sub> = O <sub>3</sub> + NO	2.0E-07	-5	0	ESTIMATED	375
376	N <sup>+</sup> + O <sub>4</sub> = O <sub>2</sub> + O <sub>2</sub> + NO	2.0E-07	-5	0	ESTIMATED	376
377	N <sup>+</sup> + CO <sub>3</sub> = NO + H <sub>2</sub> O + CO <sub>2</sub> + O	2.0E-07	-5	0	ESTIMATED	377
378	N <sup>+</sup> + 78- = CO <sub>2</sub> + O + H <sub>2</sub> O + H <sub>2</sub> O + NO	2.0E-07	-5	0	ESTIMATED	378
379	N <sup>+</sup> + CO <sub>4</sub> = CO <sub>2</sub> + NO + H <sub>2</sub> O + O <sub>2</sub>	2.0E-07	-5	0	ESTIMATED	379
380	N <sup>+</sup> + 94- = CO <sub>2</sub> + O <sub>2</sub> + H <sub>2</sub> O + H <sub>2</sub> O + NO	2.0E-07	-5	0	ESTIMATED	380
381	N <sup>+</sup> + NO <sub>2</sub> = NO + H <sub>2</sub> O + NO <sub>2</sub>	2.0E-07	-5	0	ESTIMATED	381
382	N <sup>+</sup> + 64- = NO <sub>2</sub> + H <sub>2</sub> O + NO + H <sub>2</sub> O	2.0E-07	-5	0	ESTIMATED	382
383	N <sup>+</sup> + NO <sub>3</sub> = NO + H <sub>2</sub> O + NO <sub>2</sub> + O	2.0E-07	-5	0	ESTIMATED	383
384	N <sup>+</sup> + 62- = O <sub>2</sub> + NO + NO + H <sub>2</sub> O	2.0E-07	-5	0	ESTIMATED	384
385	N <sup>+</sup> + 80- = NO <sub>2</sub> + H <sub>2</sub> O + NO + H <sub>2</sub> O + O	2.0E-07	-5	0	ESTIMATED	385
386	N <sup>+</sup> + 125- = HN03 + NO <sub>2</sub> + NO <sub>2</sub> + H <sub>2</sub> O	2.0E-07	-5	0	ESTIMATED	386
387	N <sup>+</sup> + O- = O + NO + H <sub>2</sub> O	2.0E-07	-5	0	ESTIMATED	387
388	N <sup>+</sup> + O <sub>2</sub> = NO + H <sub>2</sub> O + O <sub>2</sub>	2.0E-07	-5	0	ESTIMATED	388
389	N <sup>+</sup> + O <sub>2</sub> -W = O <sub>2</sub> + NO + H <sub>2</sub> O + H <sub>2</sub> O	2.0E-07	-5	0	ESTIMATED	389
390	N <sup>+</sup> + O <sub>3</sub> = NO + H <sub>2</sub> O + O <sub>3</sub>	2.0E-07	-5	0	ESTIMATED	390
391	N <sup>+</sup> + O <sub>4</sub> = O <sub>2</sub> + O <sub>2</sub> + H <sub>2</sub> O + O <sub>2</sub>	2.0E-07	-5	0	ESTIMATED	391
392	N <sup>+</sup> + CO <sub>3</sub> = CO <sub>2</sub> + O + NO + H <sub>2</sub> O + H <sub>2</sub> O	2.0E-07	-5	0	ESTIMATED	392
393	N <sup>+</sup> + 78- = CO <sub>2</sub> + O + H <sub>2</sub> O + H <sub>2</sub> O + H <sub>2</sub> O + NO	2.0E-07	-5	0	ESTIMATED	393
394	N <sup>+</sup> + CO <sub>4</sub> = CO <sub>2</sub> + NO + H <sub>2</sub> O + O <sub>2</sub> + H <sub>2</sub> O	2.0E-07	-5	0	ESTIMATED	394
395	N <sup>+</sup> + 94- = CO <sub>2</sub> + O <sub>2</sub> + H <sub>2</sub> O + H <sub>2</sub> O + H <sub>2</sub> O + NO	2.0E-07	-5	0	ESTIMATED	395
396	N <sup>+</sup> + NO <sub>2</sub> = NO <sub>2</sub> + H <sub>2</sub> O + H <sub>2</sub> O + NO <sub>2</sub>	2.0E-07	-5	0	ESTIMATED	396
397	N <sup>+</sup> + 64- = NO + NO <sub>2</sub> + H <sub>2</sub> O + H <sub>2</sub> O + H <sub>2</sub> O	2.0E-07	-5	0	ESTIMATED	397
398	N <sup>+</sup> + NO <sub>3</sub> = NO + H <sub>2</sub> O + H <sub>2</sub> O + NO <sub>2</sub> + O	2.0E-07	-5	0	ESTIMATED	398
399	N <sup>+</sup> + 62- = O <sub>2</sub> + NO + NO + H <sub>2</sub> O + H <sub>2</sub> O	2.0E-07	-5	0	ESTIMATED	399
400	N <sup>+</sup> + 80- = HN03 + H <sub>2</sub> O + NO + H <sub>2</sub> O + H <sub>2</sub> O + O	2.0E-07	-5	0	ESTIMATED	400
401	N <sup>+</sup> + 125- = HN03 + NO <sub>2</sub> + NO <sub>2</sub> + H <sub>2</sub> O + H <sub>2</sub> O	2.0E-07	-5	0	ESTIMATED	401
402	N <sup>+</sup> + O- = O + NO + H <sub>2</sub> O + H <sub>2</sub> O	2.0E-07	-5	0	ESTIMATED	402
403	N <sup>+</sup> + O <sub>2</sub> = NO + H <sub>2</sub> O + H <sub>2</sub> O + O <sub>2</sub>	2.0E-07	-5	0	ESTIMATED	403
404	N <sup>+</sup> + O <sub>2</sub> -W = O <sub>2</sub> + NO + H <sub>2</sub> O + H <sub>2</sub> O + H <sub>2</sub> O	2.0E-07	-5	0	ESTIMATED	404
405	N <sup>+</sup> + O <sub>3</sub> = NO + H <sub>2</sub> O + H <sub>2</sub> O + O <sub>3</sub>	2.0E-07	-5	0	ESTIMATED	405
406	N <sup>+</sup> + 78- = CO <sub>2</sub> + O <sub>2</sub> + H <sub>2</sub> O + O <sub>2</sub> + H <sub>2</sub> O	2.0E-07	-5	0	ESTIMATED	406
407	N <sup>+</sup> + CO <sub>4</sub> = CO <sub>2</sub> + NO + H <sub>2</sub> O + H <sub>2</sub> O + CO <sub>2</sub> + O	2.0E-07	-5	0	ESTIMATED	407
408	N <sup>+</sup> + 94- = CO <sub>2</sub> + O <sub>2</sub> + H <sub>2</sub> O + H <sub>2</sub> O + H <sub>2</sub> O + NO	2.0E-07	-5	0	ESTIMATED	408
409	N <sup>+</sup> + NO <sub>2</sub> = NO + H <sub>2</sub> O + H <sub>2</sub> O + H <sub>2</sub> O + O <sub>2</sub> + H <sub>2</sub> O	2.0E-07	-5	0	ESTIMATED	409
410	N <sup>+</sup> + 64- = NO + H <sub>2</sub> O + H <sub>2</sub> O + H <sub>2</sub> O + H <sub>2</sub> O + NO	2.0E-07	-5	0	ESTIMATED	410
411	N <sup>+</sup> + NO <sub>3</sub> = NO + H <sub>2</sub> O + H <sub>2</sub> O + H <sub>2</sub> O + H <sub>2</sub> O + H <sub>2</sub> O	2.0E-07	-5	0	ESTIMATED	411
412	N <sup>+</sup> + 80- = NO + H <sub>2</sub> O + H <sub>2</sub> O + H <sub>2</sub> O + H <sub>2</sub> O + O	2.0E-07	-5	0	ESTIMATED	412
413	N <sup>+</sup> + 125- = HN03 + NO <sub>2</sub> + NO <sub>2</sub> + H <sub>2</sub> O + H <sub>2</sub> O + H <sub>2</sub> O	2.0E-07	-5	0	ESTIMATED	413
414	N <sup>+</sup> + O- = O + NO + H <sub>2</sub> O + H <sub>2</sub> O + H <sub>2</sub> O + O <sub>2</sub>	2.0E-07	-5	0	ESTIMATED	414
415	N <sup>+</sup> + 80- = NO <sub>2</sub> + H <sub>2</sub> O + NO + H <sub>2</sub> O + H <sub>2</sub> O + H <sub>2</sub> O + O	2.0E-07	-5	0	ESTIMATED	415
416	N <sup>+</sup> + 125- = HN03 + NO <sub>2</sub> + NO <sub>2</sub> + H <sub>2</sub> O + H <sub>2</sub> O + H <sub>2</sub> O + H <sub>2</sub> O	2.0E-07	-5	0	ESTIMATED	416
417	N <sup>+</sup> + O- = O + NO + H <sub>2</sub> O + H <sub>2</sub> O + H <sub>2</sub> O + H <sub>2</sub> O	2.0E-07	-5	0	ESTIMATED	417
418	N <sup>+</sup> + O <sub>2</sub> = NO + H <sub>2</sub> O + O <sub>2</sub> + H <sub>2</sub> O + H <sub>2</sub> O	2.0E-07	-5	0	ESTIMATED	418
419	N <sup>+</sup> + O <sub>2</sub> -W = O <sub>2</sub> + NO + H <sub>2</sub> O + H <sub>2</sub> O + H <sub>2</sub> O + H <sub>2</sub> O	2.0E-07	-5	0	ESTIMATED	419
420	N <sup>+</sup> + O <sub>3</sub> = NO + H <sub>2</sub> O + O <sub>3</sub> + H <sub>2</sub> O + H <sub>2</sub> O + H <sub>2</sub> O	2.0E-07	-5	0	ESTIMATED	420



REAC. NO.	REACTION	A	B	C	REFERENCE	REF. NO.
481	$02 + 04 = 02 + 02 + 02$	2.0E-07	-5	0	ESTIMATED	481
482	$0250 + 03 = 02 + 02 + 02 + 0$	2.0E-07	-5	0	ESTIMATED	482
483	$0250 + 78 = 02 + 02 + 02 + 02 + 02$	2.0E-07	-5	0	ESTIMATED	483
484	$0250 + 04 = 02 + 02 + 02 + 02 + 02$	2.0E-07	-5	0	ESTIMATED	484
485	$0250 + 94 = 02 + 02 + 02 + 02 + 02$	2.0E-07	-5	0	ESTIMATED	485
486	$0250 + 02 = 02 + 02 + 02 + 02 + 02$	2.0E-07	-5	0	ESTIMATED	486
487	$0250 + 64 = 02 + 02 + 02 + 02 + 02$	2.0E-07	-5	0	ESTIMATED	487
488	$0250 + 03 = 02 + 02 + 02 + 02 + 0$	2.0E-07	-5	0	ESTIMATED	488
489	$0250 + 62 = 02 + 02 + 02 + 02 + 02$	2.0E-07	-5	0	ESTIMATED	489
490	$0250 + 80 = 02 + 02 + 02 + 02 + 02 + 0$	2.0E-07	-5	0	ESTIMATED	490
491	$0250 + 125 = 02 + 02 + 02 + 02 + 02 + 02 + 0$	2.0E-07	-5	0	ESTIMATED	491
492	$0250 + 0 = 02 + 02 + 02 + 02 + 02 + 02 + 0$	2.0E-07	-5	0	ESTIMATED	492
493	$0250 + 02 = 02 + 02 + 02 + 02 + 02 + 02 + 0$	2.0E-07	-5	0	ESTIMATED	493
494	$0250 + 02 = 02 + 02 + 02 + 02 + 02 + 02 + 0$	2.0E-07	-5	0	ESTIMATED	494
495	$0250 + 03 = 02 + 02 + 02 + 02 + 02 + 02 + 0$	2.0E-07	-5	0	ESTIMATED	495
496	$0250 + 04 = 02 + 02 + 02 + 02 + 02 + 02 + 0$	2.0E-07	-5	0	ESTIMATED	496

DATE OF LAST REACTION CHANGE IS JUNE 26, 1976

DATE OF LAST REFERENCE CHANGE IS JUNE 16, 1977